3-D Network Localization Using Angle Measurements and Reduced Communication

Liangming Chen, Kun Cao, Lihua Xie, *Fellow, IEEE*, Xiaolei Li, *Member, IEEE*, and Mir Feroskhan

***Abstract*—Other than the relative position-based and bearing-based localization with aligned coordinate frames on all sensor nodes, the existing 3D network localization algorithms using distance/bearing/angle measurements without aligned coordinate frames usually require each node to have at least four neighbors, which poses large communication burden for the network system. To reduce the communication burden in each iteration, this paper studies the 3D network localization problem where each node is allowed to have angle measurements with respect to only *three* neighbors. Firstly, we use a tetrahedral angularity to describe the network consisting of a set of nodes and tetrahedra among the nodes. Given that at least one node in each tetrahedron has the knowledge of the direction of the global Z-axis, the geometric constraint of each tetrahedron is described by an angle-induced linear constraint whose coefficient matrices are only related to the interior angles among the four nodes in the tetrahedron and the angles between the global Z-axis and the inter-node edges. Secondly, both algebraic and topological localizability conditions are derived based on the coefficient matrices of the tetrahedra's angle-induced linear constraints. Moreover, a distributed method is also presented to check the network localizability. Lastly, distributed localization laws are designed under the cases of continuous communication, aperiodic communication, and aperiodic communication on jointly localizable angularities, respectively. Simulation examples are provided to validate the effectiveness and advantages of the proposed localization laws.**

***Index Terms*—Network localization, angle measurements, angle-induced linear constraint, tetrahedral angularity, aperiodic communication, reduced communication.**

I. Introduction

RECENTLY, the network localization problem has been extensively studied due to its wide applications in practical missions, such as search and rescue [1], [2], transportation and logistics [3], [4], and reconnaissance and surveillance [5], [6]. Two classes of nodes usually exist in these networked systems, which are anchor nodes whose positions are known and free nodes whose positions are unknown [7]. The configuration of these nodes can lie in a 2D plane or 3D space. The aim of network localization is to determine the positions of the free nodes by using their measurement information with respect to their neighbors and their communication information obtained from their neighbors [8]–[10]. Therefore, these two aspects, namely sensor measurement and inter-node communication, become the main focus and evaluation factors when designing network localization algorithms for practical missions.

According to the types of sensor measurements available among the nodes, the existing network localization algorithms can be mainly classified into bearing-based, relative position-based, distance-based, and angle-based localization [8], [11]–[14]. Note that aligned bearing measurements require all free nodes' coordinate frames to have the same orientation as the anchor nodes' coordinate frames, which is challenging to be guaranteed without extra sensing, networked communication or orientation estimation. The relative position measurement consists of bearing and distance information, and thus also requires the alignment of the nodes' coordinate frames. Compared to the relative position and bearing measurements, inter-node distance measurement and triple-node angle measurement are independent to the orientations of the nodes' coordinate frames [15]–[18]. Moreover, the distance measurement and angle measurement can be acquired from sensors, such as ultra wideband and directional antenna array, respectively, which prompt the development of distance-based and angle-based localization algorithms [11], [17], [19]. The distance-based and angle-based localization algorithms have been designed in [17], [19], [20] for the case that all the nodes lie in a 2D plane. The network localization task in 3D space is more challenging which has been investigated recently in [11], [13], [21]. The proposed 3D distance-based and angle-based localization algorithms in [11], [13], [21] require each free node to have at least four neighbors, due to which the communication burden will be significantly increased when the network becomes large-scale. Therefore, it is of practical importance to further reduce the number of each node's neighbors such that not only the communication burden but also the availability of relative measurements can be reduced. However, the minimum number of neighbors required for 3D distance-based network localization is hard to be further reduced since inter-node distances are invariant to the orientations of the sensor nodes' coordinate frames.

Meanwhile, according to the continuity and frequency of the communication among nodes, the existing network localization

Manuscript received September 6, 2021; revised January 24, 2022 and March 20, 2022; accepted April 11, 2022. Date of publication April 14, 2022; date of current version May 24, 2022. The associate editor coordinating the review of this manuscript and approving it for publication was Prof. David I. Shuman. The work of Xiaolei Li was supported in part by the National Natural Science Foundation of China under Grants 61903319 and 62103352. *(Corresponding author: Mir Feroskhan.)*

Liangming Chen is with the School of Mechanical and Aerospace Engineering, Nanyang Technological University, Singapore, and also with the School of Electrical and Electronic Engineering, Nanyang Technological University, Singapore (e-mail: liangming.chen@ntu.edu.sg).

Mir Feroskhan is with the School of Mechanical and Aerospace Engineering, Nanyang Technological University, Singapore (e-mail: mir.feroskhan@ntu.edu.sg).

Kun Cao and Lihua Xie are with the School of Electrical and Electronic Engineering, Nanyang Technological University, Singapore (e-mail: kun001@e.ntu.edu.sg; elhxie@ntu.edu.sg).

Xiaolei Li is with the School of Electrical Engineering, Yanshan University, Qinhuangdao 066004, China (e-mail: 505665918@163.com).

Digital Object Identifier 10.1109/TSP.2022.3167512

algorithms can also be classified into network localization under continuous, periodic, and aperiodic communication. The communication process among nodes plays an important role in the network localization. This is because when executing network localization algorithms, the values of the sensor measurements are constant in the noiseless case which can be obtained by one time sensing and one time communication with neighbors, but the communication of estimated positions with neighbors is constantly needed over time. Most of the localization algorithms focus on the continuous communication [11], [22], [23], or periodic communication [7], [19], [20]. Very few localization algorithms focus on aperiodic communication [24], which can further reduce the communication burden. Moreover, at each sampling instant, each node needs to communicate the estimated positions with all of this neighbors in [24]. Therefore, it is also interesting to investigate the case of aperiodic communication where each node communicates with only some of its neighbors at each sampling instant.

Motivated by the aforementioned two aspects, this paper studies 3D network localization using angle measurements and reduced communication. We propose that by adding one more sensing capability for the network, namely at least one in four neighboring nodes has the knowledge of the direction of the global Z axis, each free node only needs three neighbors instead of four neighbors to construct an angle-induced linear constraint for localization. This reduces the communication burden in each iteration. Based on the established linear constraints, algebraic and topological localizability conditions are proposed. For the cases of continuous communication and aperiodic communication, distributed network localization algorithms are also designed, respectively.

The rest of this paper is organized as follows. Section II presents some preliminaries. Section III introduces angle-constrained tetrahedral angularities, based on which localizability conditions are developed in Section IV. In Section V, localization algorithms are designed under different cases. Simulation examples are provided in Section VI.

II. Preliminaries

A. Notations

Consider a 3D static sensor network consisting of $n_a \in \mathbb{N}^+$ anchor nodes and $n_f \in \mathbb{N}^+$ free nodes. Let $\mathcal{V}_a = \{1, 2, \ldots, n_a\}$ be the set of anchor nodes with $|\mathcal{V}_a| = n_a \geq 2$, whose positions, denoted by $p_a = [p_1^\top, p_2^\top, \ldots, p_{n_a}^\top]^\top \in \mathbb{R}^{3n_a}$, are known by themselves. Let $\mathcal{V}_f = \{n_a+1, n_a+2, \ldots, n\}$ be the set of free nodes with $|\mathcal{V}_f| = n_f = n - n_a$, whose positions, denoted by $p_f = [p_{n_a+1}^\top, p_{n_a+2}^\top, \ldots, p_n^\top]^\top \in \mathbb{R}^{3n_f}$, are to be determined. We assume that no colocated points exist in $p = [p_a^\top, p_f^\top]^\top \in \mathbb{R}^{3n}$. Let $I_3, 1_n, \times, \otimes, \lambda_{\max}, \lambda_{\min}$ be the 3-by-3 identity matrix, $n \times 1$ column vector of all ones, the cross product, the Kronecker product, the maximum eigenvalue, and the minimum eigenvalue of a symmetric matrix, respectively. Denote the tetrahedron formed by the nodes i, j, k, m as $\triangle ijkm$, the plane formed by three non-collinear nodes i, j, k as $\mathbb{P}_{ijk}$, respectively.

B. Angle Measurements

Let $\sum_g$ be the global coordinate frame under which p_a and p_f are represented. Each free node j holds a fixed local coordinate frame $\sum_j$ for sensor measurements whose orientation can be different from the orientation of $\sum_g$. Let p_j and p_j^i be the node j's coordinates in $\sum_g$ and $\sum_i$, respectively. Define the bearing from node j to node i by $b_{ji} := \frac{p_i - p_j}{\|p_i - p_j\|}$ which is uniquely determined by the combination of an azimuth angle and an elevation angle [25]. Then, the bearing from j to i described in $\sum_j$ can be written as $b_{ji}^j := \frac{p_i^j - p_j^j}{\|p_i^j - p_j^j\|} = Q_j b_{ji}$ where $Q_j \in SO(3)$ is the 3D rotation matrix describing the rotation from $\sum_g$ to $\sum_j$. Then, the angle α_{ijk} between the rays $\overrightarrow{ji}$ and $\overrightarrow{jk}$ can be calculated by

$$\alpha_{ijk} := \arccos(b_{ji}^\top b_{jk}) \in [0, \pi]. \tag{1}$$

Due to the facts that $Q_j^\top Q_j = I_3$ and $\arccos(b_{ji}^{j\top} b_{jk}^j) = \arccos(b_{ji}^\top Q_j^\top Q_j b_{jk}) = \arccos(b_{ji}^\top b_{jk})$, the angle α_{ijk} has the same value in $\sum_j$ and $\sum_g$. This also holds for the angle formed by $\overrightarrow{ji}$ and $\mathbb{P}_{mjk}$, i.e., $\arccos(b_{ji}^{j\top} \frac{b_{jk}^j \times b_{jm}^j}{\|b_{jk}^j \times b_{jm}^j\|}) = \arccos(b_{ji}^\top Q_j^\top Q_j \frac{b_{jk} \times b_{jm}}{\|b_{jk} \times b_{jm}\|}) = \arccos(b_{ji}^\top \frac{b_{jk} \times b_{jm}}{\|b_{jk} \times b_{jm}\|})$. We assume in this paper that each sensor node $j \in \mathcal{V}_f$ has the knowledge of the angles α_{ijk} and $\arccos(b_{ji}^\top \frac{b_{jk} \times b_{jm}}{\|b_{jk} \times b_{jm}\|}), i, k, m \in \mathcal{N}_j$, where $\mathcal{N}_j$ denotes node j's neighbor set. In practice, these two angles usually are indirectly calculated from those azimuth and elevation angles which are the original measured angles from sensors, such as cameras and directional antenna arrays. For brevity, we also say in this paper that α_{ijk} and $\arccos(b_{ji}^\top \frac{b_{jk} \times b_{jm}}{\|b_{jk} \times b_{jm}\|})$ are measured angles. In addition, if a node i has the knowledge of the global Z axis, then i can additionally measure the angle between the global Z axis and the ray $\overrightarrow{ik}, k \in \mathcal{N}_i$.

III. Angle-Constrained Sensor Networks

In this section, we first introduce an angle-induced linear constraint for a tetrahedron with 4 neighboring sensor nodes as its vertices, then use tetrahedral angularities to describe those sensor networks with multiple tetrahedra, finally investigate their properties by defining an angle measurement matrix.

A. Angle-Induced Linear Constraint in a Tetrahedron

According to [13], [20], describing geometric constraints among sensor nodes as linear algebraic equations is an efficient way to solve network localization problems. Therefore, we first aim to establish an angle-induced linear constraint for a basic geometric unit in the 3D sensor network, namely a 4-node tetrahedron. Consider a tetrahedron formed by four non-coplanar nodes 1,2,3,4, which is denoted by $\triangle 1234$. Note that most of the established distance-induced [21], bearing-induced [14], [20], angle-induced [11], [12] linear constraints have scalar coefficients and associate with 5 neighboring nodes in 3D. Instead, we now prove that a 3D angle-induced linear constraint's coefficients in front of the 4 nodes' positions

p_1, p_2, p_3, p_4 should not be all scalars. Suppose on the contrary that there exists a linear representation $p_1 = ap_2 + bp_3 + cp_4$ where a, b, c are nonzero scalars. Since the translational transformation $\{p_1 + 1_3, p_2 + 1_3, p_3 + 1_3, p_4 + 1_3\}$ should also satisfy the linear representation, which indicates $a + b + c = 1$. Then, the linear representation can be rewritten as

$$a(p_2 - p_1) + b(p_3 - p_1) + c(p_4 - p_1) = 0 \tag{2}$$

Since $\frac{b}{a}, \frac{c}{a}$ are scalars, (2) indicates that $\{p_1, p_2, p_3, p_4\}$ must be co-planar, which contradicts with the assumption that p_1, p_2, p_3, p_4 are non-coplanar.

Therefore, when p_1, p_2, p_3, p_4 are non-coplanar, at least one coefficient in front of p_1, p_2, p_3, p_4 in the linear constraint to be developed must be a non-zero matrix. Inspired by [20], we firstly construct $\triangle 1234$'s similar tetrahedron[1] $\triangle 1'2'3'4'$ by using the information of available angle measurements where $1', 2', 3',$ and $4'$ are four virtually constructed nodes. Then, we need to calculate the coefficient matrices in the linear constraint to be developed. The construction of the similar tetrahedron and calculation of the matrices are given in three steps.

Step 1 (assign coordinate frames): Let 1 and $1'$ be coincident. Assume that node 1 is the node that has the knowledge of the global Z-axis, and node 1's Z-axis is aligned with the global Z-axis. Since $\sum_g$ is unavailable for other nodes, we define a new coordinate frame $\sum_{1'-X_0Y_0Z_0}$ to describe the coordinates of $1', 2', 3',$ and $4'$, where the origin of $\sum_{1'-X_0Y_0Z_0}$ is $1'$. Then, we choose node 1's Z-axis as the direction of Z_0-axis. Since at least one of p_2, p_3, p_4 will not lie in the line $1Z_0$ (otherwise the four nodes are coplanar), without loss of generality, we assume p_2 is not in the line $1Z_0$. Then, we choose Y_0-axis such that $\mathbb{P}_{2'1'Z_0}$ coincides with $\mathbb{P}_{Y_0 1' Z_0}$ and $b_{1'2'}^\top b_{1'Y_0} > 0$ (this is used to exclude the case that $2'$ lies in the right side of $\mathbb{P}_{X_0 1' Z_0}$). Then, the direction of X_0-axis can be determined by the right-hand rule. Note that rotating $\triangle 1234$ along the Z_0-axis can yield $\triangle 1'2'3'4'$.

Step 2 (calculate coordinates of the similar tetrahedron): Denote by $q_{1'}, q_{2'}, q_{3'}, q_{4'}$ the coordinates of $1'$, $2'$, $3'$, and $4'$ in $\sum_{1'-X_0Y_0Z_0}$, respectively. Suppose that the scale of $\triangle 1'2'3'4'$ is determined by $l_{1'2'} = \|q_{1'} - q_{2'}\|$ and without loss of generality we assume $l_{1'2'} = 1$, which will not affect the linear constraint since $\triangle 1234$, $\triangle 1'2'3'4'$ are only required to be similar. Since $q_{1'} = [0, 0, 0]^\top$, we can calculate the remaining coordinates $q_{2'}, q_{3'}, q_{4'}$ using only angle measurements. Using the fact $b_{1'2'}^\top b_{1'Y_0} > 0$, one has

$$q_{2'} = [0, \sin\alpha_{2'1'Z_0}, \cos\alpha_{2'1'Z_0}]^\top, \tag{3}$$

where $\alpha_{2'1'Z_0} = \arccos(b_{1'2'}^\top b_{1'Z_0}) = \arccos(b_{12}^\top b_{1Z_0}) = \alpha_{21Z_0}$ can be obtained by node 1's angle measurement. Since $l_{1'2'} = 1$, using the Law of Sines, one has $l_{1'3'} = \frac{\sin\alpha_{1'2'3'}}{\sin\alpha_{1'3'2'}}$. Suppose that node 3's coordinate is $q_{3'} = [x_{3'}, y_{3'}, z_{3'}]^\top$. Then, we can firstly obtain

$$z_{3'} = l_{1'3'}\cos\alpha_{Z_0 1'3'} = \sin\alpha_{123}\cos\alpha_{Z_0 13}/\sin\alpha_{132} \tag{4}$$

To calculate $x_{3'}, y_{3'}$, as shown in Fig. 1, we define three points H_1, H_2, H_3 which satisfy $H_1 \in \mathbb{P}_{X_0 1' Y_0}, 3'H_1 \perp 1'H_1, H_2 \in$

[1]Two tetrahedra are said to be similar here if all the corresponding interior angles and the sign of the signed volume of the two tetrahedra are the same.

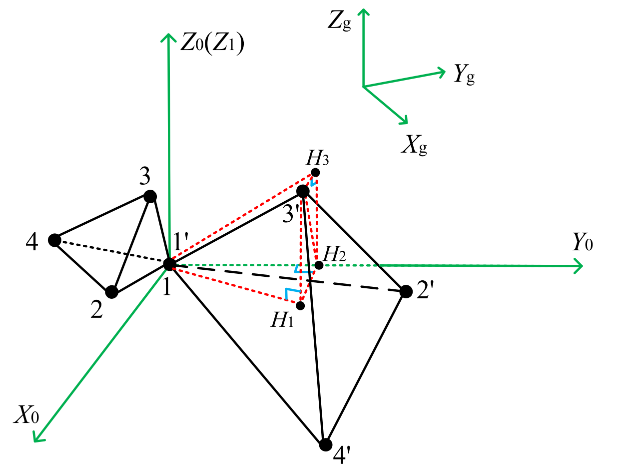

Fig. 1. Construction of a similar tetrahedron $\triangle 1'2'3'4'$ from $\triangle 1234$.

$\mathbb{P}_{X_0 1' Y_0} \cap \mathbb{P}_{Y_0 1' Z_0}$, $H_1H_2 \perp 1'Y_0$, $H_3 \in \mathbb{P}_{Y_0 1' Z_0}$, and $3'H_3 \perp 1'H_3$. Since $\alpha_{3'1'H_3}$ is the angle formed by $1'3'$ and $\mathbb{P}_{2'1'Z_0}$, one has $l_{3'H_3} = l_{1'3'}\sin\alpha_{H_3 1'3'} = l_{1'3'}\left|b_{3'1'}^\top \frac{b_{1'Z_0}\times b_{1'2'}}{\|b_{1'Z_0}\times b_{1'2'}\|}\right|$. It follows that $l_{H_1H_2} = l_{3'H_3}$ and $l_{1'H_2} = \sqrt{l_{1'3'}^2 - z_{3'}^2 - l_{H_1H_2}^2}$. According to the geometric relation in Fig. 1, one has the remaining coordinates of point 3'

$$x_{3'} = \begin{cases} l_{H_1H_2}, \text{if } b_{1'3'}^\top (b_{1'2'} \times b_{1'Z_0}) > 0, \\ -l_{H_1H_2}, \text{otherwise}, \end{cases} \tag{5}$$

$$y_{3'} = \begin{cases} l_{1'H_2}, \text{if } b_{1'3'}^\top \bar{b}_{1'H_2} > 0, \\ -l_{1'H_2}, \text{otherwise}, \end{cases} \tag{6}$$

where $\bar{b}_{1'H_2} = \begin{bmatrix}1,0,0\\0,1,0\\0,0,0\end{bmatrix} b_{1'2'}$, and $b_{1'3'}^\top \bar{b}_{1'H_2} = b_{13}^\top \begin{bmatrix}1,0,0\\0,1,0\\0,0,0\end{bmatrix} b_{12}$ can be obtained from node 1's angle measurements (we have used $R_z^\top(\theta)R_z(\theta) = I_3$ for arbitrary θ), and $b_{1'3'}^\top (b_{1'2'} \times b_{1'Z_0})$ has the same sign as $b_{1'3'}^\top \frac{b_{1'2'}\times b_{1'Z_0}}{\|b_{1'2'}\times b_{1'Z_0}\|}$. Since $\|b_{1'Z_0} \times b_{1'2'}\| \neq 0$, the above calculation is well-defined.

Similar to the calculation of the coordinates of point 3', one can also calculate the coordinates of point 4', which we denote as $q_{4'} = [x_{4'}, y_{4'}, z_{4'}]^\top$. Following (4)–(6), one has

$$z_{4'} = l_{1'4'}\cos\alpha_{Z_0 1'4'}, \tag{7}$$

$$x_{4'} = \begin{cases} l_{H_4H_5}, \text{if } b_{1'4'}^\top (b_{1'2'} \times b_{1'Z_0}) > 0, \\ -l_{H_4H_5}, \text{otherwise}, \end{cases} \tag{8}$$

$$y_{4'} = \begin{cases} l_{1'H_5}, \text{if } b_{1'4'}^\top b_{1'H_5} > 0, \\ -l_{1'H_5}, \text{otherwise}, \end{cases} \tag{9}$$

where $l_{1'4'} = l_{1'3'}\frac{\sin\alpha_{1'3'4'}}{\sin\alpha_{1'4'3'}}$, the points H_4, H_5, H_6 are used to calculate the coordinates of $4'$ and are similarly constructed as these points H_1, H_2, H_3, respectively, and thus $l_{4'H_6} = l_{1'4'}\sin\alpha_{H_6 1'4'} = l_{1'4'}\left|b_{4'1'}^\top \frac{b_{1'Z_0}\times b_{1'2'}}{\|b_{1'Z_0}\times b_{1'2'}\|}\right|$, $l_{H_4H_5} = l_{4'H_6}$ and $l_{1'H_5} = \sqrt{l_{1'4'}^2 - z_{4'}^2 - l_{H_4H_5}^2}$, and $b_{1'H_5} = b_{1'H_2}$.

Step 3 (construct the angle-induced linear constraint): After knowing the coordinates of $1', 2', 3'$, and $4'$ in $\sum_{1'-X_0Y_0Z_0}$, we now construct the angle-induced linear constraint for the tetrahedron $\triangle 1234$ in $\sum_g$. According to Step 1, one has the relationship between p_i and $q_{i'}$

$$p_i = k_s R_z(\theta) q_{i'} + w, \forall i = 1,2,3,4, \tag{10}$$

where $k_s \in \mathbb{R}^+$ is the scaling factor from $\triangle 1'2'3'4'$ to $\triangle 1234$, $w \in \mathbb{R}^3$ is the translation vector from $1'$ to 1 described in $\sum_g$, and $R_z(\theta) = \left[\begin{smallmatrix}\cos\theta & -\sin\theta & 0\\ \sin\theta & \cos\theta & 0\\ 0 & 0 & 1\end{smallmatrix}\right]$ represents the Z-axis rotation with rotation angle $\theta \in [0, 2\pi)$ from $\triangle 1'2'3'4'$ to $\triangle 1234$, respectively. Therefore, if a linear constraint can be established for $\triangle 1'2'3'4'$ in $\sum_{1'-X_0Y_0Z_0}$ and it is invariant with respect to the tetrahedron $\triangle 1'2'3'4'$'s scaling k_s, translation $w \in \mathbb{R}^3$ and rotation $R_z(\theta)$, then that linear constraint also holds for the tetrahedron $\triangle 1234$ in $\sum_g$. Based on this fact, we firstly aim to establish a linear constraint for $\triangle 1'2'3'4'$ in $\sum_{1'-X_0Y_0Z_0}$. We assume that the constraint can be written as

$$\begin{aligned}&[a_1,\ a_2,\ a_3]q_{1'} + [b_1,\ b_2,\ b_3]q_{2'}\\ &+ [c_1,\ c_2,\ c_3]q_{3'} + [\ d_2,\ d_3]q_{4'} = 0,\end{aligned} \tag{11}$$

where $a_i \in \mathbb{R}, b_i \in \mathbb{R}, c_i \in \mathbb{R}$, and $d_i \in \mathbb{R}, i = 1,2,3$. Then, we need to calculate the coefficients a_i, b_i, c_i, d_i using the condition that (11) always holds under $\triangle 1'2'3'4'$'s translation motion, scaling motion, and rotation motion along the Z-axis. Firstly, for the case of translation motion, one has that for $\forall w \in \mathbb{R}^3$,

$$\begin{aligned}&[a_1,\ a_2,\ a_3](q_{1'} + w) + [b_1,\ b_2,\ b_3](q_{2'} + w)\\ &+ [c_1,\ c_2,\ c_3](q_{3'} + w)\\ &+ [d_1,\ d_2,\ d_3](q_{4'} + w) = 0.\end{aligned} \tag{12}$$

Substituting the cases of $w = [1,0,0]^\top, w = [0,1,0]^\top, w = [0,0,1]^\top$ into (12), respectively, yields

$$a_i + b_i + c_i + d_i = 0, \forall i = 1,2,3. \tag{13}$$

Since $a_i = -(b_i + c_i + d_i)$, (11) can be rewritten as

$$\begin{aligned}&\begin{bmatrix}b_1, & b_2, & b_3\end{bmatrix}(q_{2'} - q_{1'}) + \begin{bmatrix}c_1, & c_2, & c_3\end{bmatrix}(q_{3'} - q_{1'})\\ &+ \begin{bmatrix}d_1, & d_2, & d_3\end{bmatrix}(q_{4'} - q_{1'}) = 0.\end{aligned} \tag{14}$$

Secondly, for the case of scaling motion, one has that (14) holds. Lastly, for the case of rotation motion along the Z-axis, one has

$$\begin{aligned}&[b_1, b_2, b_3]R_z(\theta)(q_{2'} - q_{1'}) + [c_1, c_2, c_3]R_z(\theta)(q_{3'} - q_{1'})\\ &+ \begin{bmatrix}d_1, & d_2, & d_3\end{bmatrix}R_z(\theta)(q_{4'} - q_{1'}) = 0, \forall\theta \in [0, 2\pi).\end{aligned} \tag{15}$$

Substituting the definition of $R_z(\theta)$ into (15) yields

$$f_1 \cos\theta + f_2 \sin\theta + f_3 = 0, \tag{16}$$

where

$$\begin{aligned}f_1 &= b_1 q_{2'}(1) + b_2 q_{2'}(2) + c_1 q_{3'}(1)\\ &\quad + c_2 q_{3'}(2) + d_1 q_{4'}(1) + d_2 q_{4'}(2)\\ f_2 &= b_2 q_{2'}(1) - b_1 q_{2'}(2) + c_2 q_{3'}(1)\\ &\quad - c_1 q_{3'}(2) + d_2 q_{4'}(1) - d_1 q_{4'}(2)\\ f_3 &= b_3 q_{2'}(3) + c_3 q_{3'}(3) + d_3 q_{4'}(3),\end{aligned}$$

and $q_{i'}(j)$ is the jth component of $q_{i'}$, and we have used the fact $q_{1'} = [0,0,0]$. Since (16) should hold for $\forall\theta \in [0, 2\pi)$, one must have $f_1 = 0, f_2 = 0, f_3 = 0$. Note that $\{f_1 = 0, f_3 = 0\}$ are linearly dependent to (14). Therefore, we can only obtain two linearly independent constraints $f_1 = 0, f_2 = 0$ for the case of the rotation motion. To sum up, the linear constraint (14) should satisfy two linearly independent constraints, namely $f_1 = 0$ and $f_2 = 0$, which can be written into a compact form

$$S\begin{bmatrix}b_1, b_2, b_3, c_1, c_2, c_3, d_1, d_2, d_3\end{bmatrix}^\top = 0, \tag{17}$$

where the matrix S is shown at the bottom of this page.

Now, we discuss the rank of the matrix $S \in \mathbb{R}^{3\times 9}$. Suppose that the first row and second row of S are linearly dependent. It follows that $q_{i'}(1) = q_{i'}(2) = 0, \forall i = 2,3,4$ which contradicts to the fact that $\triangle 1'2'3'4'$ is non-coplanar. Since the third row of S is linearly independent to the first two rows, the three rows of S are linearly independent. Applying the same reasoning to the columns of S yields that there exist at least three linearly independent columns in S. Combining these two aspects, one has that $\mathrm{Rank}(S) = 3$.

Since the rank of the matrix S is 3, the null space of S is spanned by six linearly independent vectors, i.e., $[b_1, b_2, b_3, c_1, c_2, c_3, d_1, d_2, d_3]$ has six linearly independent solutions satisfying (17). Substituting the six linearly independent solutions of $[b_1, b_2, b_3, c_1, c_2, c_3, d_1, d_2, d_3]$ into (14) and writing them into a compact matrix form yield

$$\begin{aligned}&B_{12}(\alpha)(q_{2'} - q_{1'}) + C_{13}(\alpha)(q_{3'} - q_{1'})\\ &+ D_{14}(\alpha)(q_{4'} - q_{1'}) = 0,\end{aligned} \tag{18}$$

where $B_{12}(\alpha) \in \mathbb{R}^{6\times 3}, C_{13}(\alpha) \in \mathbb{R}^{6\times 3}, D_{14}(\alpha) \in \mathbb{R}^{6\times 3}$ are the row stacks of the six solutions of $[b_1, b_2, b_3] \in \mathbb{R}^{1\times 3}$, $[c_1, c_2, c_3] \in \mathbb{R}^{1\times 3}$, $[d_1, d_2, d_3] \in \mathbb{R}^{1\times 3}$, respectively, which are the functions of the angle measurements. Using the relationship (10) and the fact that (18) is invariant with respect to the tetrahedron $\triangle 1'2'3'4'$'s scaling motion k_s, translation motion $w \in \mathbb{R}^3$ and rotation motion $R_z(\theta)$, one has that the linear constraint for

$$S = \begin{bmatrix} q_{2'}(1) & q_{2'}(2) & 0 & q_{3'}(1) & q_{3'}(2) & 0 & q_{4'}(1) & q_{4'}(2) & 0\\ -q_{2'}(2) & q_{2'}(1) & 0 & -q_{3'}(2) & q_{3'}(1) & 0 & -q_{4'}(2) & q_{4'}(1) & 0\\ 0 & 0 & q_{2'}(3) & 0 & 0 & q_{3'}(3) & 0 & 0 & q_{4'}(3)\end{bmatrix} \in \mathbb{R}^{3\times 9}.$$

Algorithm 1: Construct an Angle-Induced Linear Constraint For Non-Coplanar $\triangle 1234$ where Z_1 is Aligned With Z_g and p_2 is Not in The Line $1Z_g$.

Input: Node 1's angle measurements with respect to its neighboring nodes and Z-axis, nodes 2's, 3's, and 4's angle measurements with respect to their neighboring nodes

Step 1 Assign the coordinate frame $\sum_{1'-X_0Y_0Z_0}$ with node 1 as its origin

Step 2: Calculate the vertices' coordinates of the similar tetrahedron $\triangle 1'2'3'4'$ by using (3)–(9)

Step 3: Construct matrix S using its definition after (17), calculate six linearly independent vectors lying in the null space of S, write these six column vectors in the form of $[B_{12}, C_{13}, D_{14}]^\top$

Output: The angle-induced linear constraint can be written as (19)

the tetrahedron $\triangle 1234$ in $\sum_g$ can be written as

$$A_1(\alpha)p_1 + B_{12}(\alpha)p_2 + C_{13}(\alpha)p_3 + D_{14}(\alpha)p_4 = 0, \quad (19)$$

where $A_1(\alpha) = -B_{12}(\alpha) - C_{13}(\alpha) - D_{14}(\alpha)$. Since $B_{12}(\alpha), C_{13}(\alpha), D_{14}(\alpha)$ are calculated using only angle measurements, the established linear constraint (19) can be constructed for the tetrahedron $\triangle 1234$ in $\sum_g$ using angle-only measurements in each node's local coordinate frame. Now, we summarize the above construction steps into Algorithm 1.

Then, we provide a numerical example to illustrate the above calculation steps 1 to 3.

Example 1: Consider four nodes 1,2,3,4 embedding in $p_1 = [3, 5, 8]^\top, p_2 = [2.281, 5.678, 7.845]^\top, p_3 = [2.199, 4.534, 7.580]^\top, p_4 = [1.121, 11.170, -7.500]^\top$, and Z_1 is aligned with the global Z-axis. Using (3)–(9), the coordinates of 1', 2', 3', and 4' described in $\sum_{1'-X_0Y_0Z_0}$ are $q_{1'} = [0, 0, 0]^\top, q_{2'} \approx [0, 0.899, 0.437]^\top, q_{3'} \approx [-0.447, 0.666, -0.626]^\top, q_{4'} \approx [-3.125, 0.172, 0.961]^\top$. Using Step 3, one has $A_1 \approx \begin{bmatrix} -11.09 & -2.10 & 0 \\ 2.10 & -11.09 & 0 \\ 0 & 0 & -9.45 \\ 6.00 & -4.03 & 0 \\ 4.03 & 6.00 & 0 \\ 0 & 0 & 10.16 \end{bmatrix}$, $B_{12} \approx \begin{bmatrix} 1.172 & 0.777 & 0 \\ -0.777 & 1.172 & 0 \\ 0 & 0 & -0.271 \\ -7.133 & 6.700 & 0 \\ -6.700 & -7.133 & 0 \\ 0 & 0 & -9.996 \end{bmatrix}$,

$C_{13} \approx \begin{bmatrix} 9.807 & -0.029 & 0 \\ 0.029 & 9.807 & 0 \\ 0 & 0 & 9.993 \\ 0.505 & -1.264 & 0 \\ 1.264 & 0.505 & 0 \\ 0 & 0 & -0.268 \end{bmatrix}$, and $D_{14} \approx \begin{bmatrix} 0.112 & 1.356 & 0 \\ -1.356 & 0.112 & 0 \\ 0 & 0 & -0.268 \\ 0.633 & -1.404 & 0 \\ 1.404 & 0.633 & 0 \\ 0 & 0 & 0.108 \end{bmatrix}$. Following (19), the angle-induced linear constraint can be constructed as

$$A_1p_1 + B_{12}p_2 + C_{13}p_3 + D_{14}p_4 = 0 \quad (20)$$

which can be verified by substituting the coordinates of $p_i, i = 1, \ldots, 4$ and $A_1, B_{12}, C_{13}, D_{14}$ into the left side of (20). Since the left side of (20) is indeed zero, this example validates the correctness of (19). □

Now, we introduce a lemma about these four matrices.

Lemma 1: For a tetrahedron $\triangle 1234$, if its vertices are non-coplanar and the matrices $A_1(\alpha), B_{12}(\alpha), C_{13}(\alpha), D_{14}(\alpha)$ are constructed according to Algorithm 1, then the kernel of the matrix $F = [A_1(\alpha), B_{12}(\alpha), C_{13}(\alpha), D_{14}(\alpha)] \in \mathbb{R}^{6\times 12}$ is spanned by six linearly independent vectors, or equivalently, *Rank*$(F) = 6$.

Proof: Firstly, according to (17), one has that $\left[b_1, b_2, b_3, c_1, c_2, c_3, d_1, d_2, d_3\right] S^\top = 0$ holds for all the six solutions of $[b_1, b_2, b_3, c_1, c_2, c_3, d_1, d_2, d_3]$, i.e., $[B_{12}(\alpha), C_{13}(\alpha), D_{14}(\alpha)]S^\top = 0$. Then, one has that

$$[A_1(\alpha), B_{12}(\alpha), C_{13}(\alpha), D_{14}(\alpha)] \begin{bmatrix} 0_{3\times 3} \\ S^\top \end{bmatrix} = 0 \quad (21)$$

which implies that all the three column vectors of $\left[\begin{smallmatrix} 0_{3\times 3} \\ S^\top \end{smallmatrix}\right] \in \mathbb{R}^{12\times 3}$ lie in the null space of F.

Secondly, according to (18), one has $B_{12}(\alpha)q_{2'} + C_{13}(\alpha)q_{3'} + D_{14}(\alpha)q_{4'} = 0$. Since $A_1(\alpha) = -B_{12}(\alpha) - C_{13}(\alpha) - D_{14}(\alpha)$, one has that for every $i = 1, 2, 3$,

$$A_1(\alpha)e_i + B_{12}(\alpha)(q_{2'} + e_i) + C_{13}(\alpha)(q_{3'} + e_i) + D_{14}(\alpha)(q_{4'} + e_i) = 0,$$

where $e_1 = [1, 0, 0]^\top, e_2 = [0, 1, 0]^\top, e_3 = [0, 0, 1]^\top$. It follows that the three column vectors $[e_i; q_{2'} + e_i; q_{3'} + e_i; q_{4'} + e_i], \forall i = 1, 2, 3$ also lie in the null space of F.

Lastly, all the six column vectors, including $\left[\begin{smallmatrix} 0_{3\times 3} \\ S^\top \end{smallmatrix}\right]$ and $[e_i; q_{2'} + e_i; q_{3'} + e_i; q_{4'} + e_i], i = 1, 2, 3$ are linearly independent with each other since $e_i \neq 0$. Moreover, $[B_{12}(\alpha), C_{13}(\alpha), D_{14}(\alpha)]$ is linearly column independent according to (17). Therefore, Rank$(F) = 6$. ■

Lemma 1 provides a necessary condition for a tetrahedron to be non-coplanar. The condition (i.e., Rank$(F) = 6$) in Lemma 1 is not sufficient for the tetrahedron to be non-coplanar. This is because if Rank$(F) = 6$, i.e., Rank$(S) = 3$, then the tetrahedron $\triangle 1'2'3'4'$ may still be coplanar. A simple example is $q_{1'} = [0; 0; 0], q_{2'} = [0.5; 1; 2], q_{3'} = 2 * [0.5; 1; 2], q_{4'} = 3 * [0.5; 1; 2]$. It can be verified that Rank$(S) = 3$, but $1', 2', 3'$, and $4'$ are collinear. After the establishment of angle-induced linear constraint for one tetrahedron, we now investigate the network case which includes multiple tetrahedra and multiple angle-induced linear constraints.

B. Tetrahedral Angularity

Angle rigidity has been investigated in [16], [26] where the notion of *angularity* is defined to describe those frameworks with triple-vertex angle constraints. Here, we briefly review some related definitions in 3D and more details can be found in [16], [26]. For the vertex set $\mathcal{V} = \{1, 2, \ldots, n\}$, define a three-vertex *triplet* (i, j, k) to describe the angle constraint α_{ijk}. Then, we define $\mathcal{A} \subseteq \mathcal{V} \times \mathcal{V} \times \mathcal{V} = \{(i, j, k), i, j, k \in \mathcal{V}, i \neq j \neq k\}$ as an angle set, each element of which is a triplet. We say (j, i, k) and (k, i, j) are conjugate triplets. We assume that $\mathcal{A}$ does not contain conjugate triplets, and (j, i, k) can be freely changed to

(k, i, j) for a given $\mathcal{A}$. Then, the combination of the vertex set $\mathcal{V}$, the angle set $\mathcal{A}$ and the position configuration $p \in \mathbb{R}^{3n}$ is called an *angularity* which we denote by $\mathbb{A}(\mathcal{V}, \mathcal{A}, p)$. Without p, the combination of the vertex set $\mathcal{V}$ and the angle set $\mathcal{A}$ is called a *trigraph* $\mathcal{T}(\mathcal{V}, \mathcal{A})$.

We say $\mathcal{A}$ is a *triangular angle set* if for every $(i_1, j_1, k_1) \in \mathcal{A}$, there also exists $\{(j_1, k_1, i_1), (k_1, i_1, j_1)\} \subset \mathcal{A}$. Then, a triangular angle set $\mathcal{A}$ can be written in the form of

$$\mathcal{A} = \{\cdots, (i_1, j_1, k_1), (j_1, k_1, i_1), (k_1, i_1, j_1), \cdots\} \tag{22}$$

and $\mathcal{S}_{\triangle i_1 j_1 k_1} = \{(i_1, j_1, k_1), (j_1, k_1, i_1), (k_1, i_1, j_1)\}$ denotes as the triangular angle set of $\triangle i_1 j_1 k_1$. Then, we say $\mathcal{A}$ is a *tetrahedral angle set* if $\mathcal{A}$ is a triangular angle set and for every triangular angle subset $\mathcal{S}_{\triangle i_1 j_1 k_1} \in \mathcal{A}$, there always exists a vertex $m \in \mathcal{V}, m \neq i \neq j \neq k$ such that $\mathcal{S}_{\triangle i_1 j_1 m} \in \mathcal{A}, \mathcal{S}_{\triangle i_1 k_1 m} \in \mathcal{A}, \mathcal{S}_{\triangle j_1 k_1 m} \in \mathcal{A}$. Then, a tetrahedral angle set $\mathcal{A}$ can be written in the form of

$$\mathcal{A} = \{\cdots, \mathcal{S}_{\triangle i_1 j_1 k_1}, \mathcal{S}_{\triangle i_1 j_1 m}, \mathcal{S}_{\triangle i_1 k_1 m}, \mathcal{S}_{\triangle j_1 k_1 m}, \cdots\} \tag{23}$$

and we denote the corresponding tetrahedral angle set of $\bigtriangleup i_1 j_1 k_1 m$ as $\mathcal{S}_{\bigtriangleup i_1 j_1 k_1 m} = \{\mathcal{S}_{\triangle i_1 j_1 k_1}, \mathcal{S}_{\triangle i_1 j_1 m}, \mathcal{S}_{\triangle i_1 k_1 m}, \mathcal{S}_{\triangle j_1 k_1 m}\}$. We say $\mathbb{A}(\mathcal{V}, \mathcal{A}, p)$ is a *tetrahedral angularity* and $\mathcal{T}(\mathcal{V}, \mathcal{A})$ a *tetrahedral trigraph* if $\mathcal{A}$ is a tetrahedral angle set. Denote by $n_{\mathcal{A}}^{\bigtriangleup} \in \mathbb{N}^+$ the total number of tetrahedron in the tetrahedral trigraph $\mathcal{T}$. Given $\mathcal{S}_{\bigtriangleup ijkm} \in \mathcal{A}$, define a matrix-weighted vector function of p_i, p_j, p_k, p_m as

$$\begin{aligned} f^{\bigtriangleup ijkm}(\alpha^*, p) &:= A^{\bigtriangleup ijkm}(\alpha^*) p_i + B^{\bigtriangleup ijkm}(\alpha^*) p_j \\ &\quad + C^{\bigtriangleup ijkm}(\alpha^*) p_k + D^{\bigtriangleup ijkm}(\alpha^*) p_m, \end{aligned} \tag{24}$$

where $f^{\bigtriangleup ijkm}(\alpha^*, p) \in \mathbb{R}^{6\times 1}$, and constant matrices $B^{\bigtriangleup ijkm}(\alpha^*)$, $C^{\bigtriangleup ijkm}(\alpha^*)$, $D^{\bigtriangleup ijkm}(\alpha^*)$ are defined according to the calculation in Algorithm 1, α^* represents those angles that are associated with the construction of (19), and $A^{\bigtriangleup ijkm}(\alpha^*) = -B^{\bigtriangleup ijkm}(\alpha^*) - C^{\bigtriangleup ijkm}(\alpha^*) - D^{\bigtriangleup ijkm}(\alpha^*)$. Note that if the constant angles α^* are calculated under p, one directly has $f^{\bigtriangleup ijkm}(\alpha^*(p), p) = 0$.

C. Angle Measurement Matrix

For the tetrahedral angularity $\mathbb{A}(\mathcal{V}, \mathcal{A}, p)$, we define the *tetrahedral angle function*

$$f_{\mathcal{A}}(p) := [\cdots, \left(f^{\bigtriangleup ijkm}(\alpha^*, p)\right)^\top, \cdots]^\top \in \mathbb{R}^{6 n_{\mathcal{A}}^{\bigtriangleup}},$$

where $\mathcal{S}_{\bigtriangleup ijkm} \in \mathcal{A}$, α^* in $A^{\bigtriangleup ijkm}, B^{\bigtriangleup ijkm}$, $C^{\bigtriangleup ijkm}$, $D^{\bigtriangleup ijkm}$ represents the angle constraints associated with $\bigtriangleup ijkm$. Since $f^{\bigtriangleup ijkm}(\alpha^*(p), p) = 0$, one has

$$R_{\mathcal{A}}(\alpha(p)) p = 0, \tag{25}$$

where $R_{\mathcal{A}}(\alpha) \in \mathbb{R}^{6 n_{\mathcal{A}}^{\bigtriangleup} \times 3n}$ is defined as the *angle measurement matrix* in 3D which can be written as

$$\begin{array}{c} \\ 1\text{st}\bigtriangleup \\ \cdots \\ \bigtriangleup_{ijkm} \\ \cdots \\ n_{\mathcal{A}}^{\bigtriangleup}\text{th}\bigtriangleup \end{array} \begin{array}{c} \begin{array}{cccccc} \cdots & \text{Vertex } i & \text{Vertex } j & \text{Vertex } k & \text{Vertex } m & \cdots \end{array} \\ \begin{bmatrix} \cdots & \cdots & \cdots & \cdots & \cdots & \cdots \\ \cdots & \cdots & \cdots & \cdots & \cdots & \cdots \\ 0 & A^{\bigtriangleup ijkm} & B^{\bigtriangleup ijkm} & C^{\bigtriangleup ijkm} & D^{\bigtriangleup ijkm} & 0 \\ \cdots & \cdots & \cdots & \cdots & \cdots & \cdots \\ \cdots & \cdots & \cdots & \cdots & \cdots & \cdots \end{bmatrix} \end{array}$$

whose row blocks are indexed by the tetrahedra defined in $\mathcal{A}$, and column blocks are indexed by the vertices in $\mathcal{V}$. It is worth noting that different from the angle rigidity matrix defined in [16, Eqn. 13], the angle measurement matrix $R_{\mathcal{A}}(\alpha)$ is only related with the values of those constrained angles defined in $\mathcal{A}$ and some additional angles between the global *Z*-axis and inter-node edges, but not related with sensor nodes' position information p or inter-node distance information, which plays an important role in this network localization problem. Given $\mathcal{V}$ and its embedding p, we define $\mathcal{A}^* := \{(i, j, k), \forall i, j, k \in \mathcal{V}, i \neq j \neq k\}$ as the complete angle set, and define $\mathbb{A}^*(\mathcal{V}, \mathcal{A}^*, p)$ and $R_{\mathcal{A}^*}$ as the corresponding tetrahedral angularity and angle measurement matrix, respectively. According to the structure of matrix S for a 4-node tetrahedron, we now define a new matrix $K_{\mathbb{A}}$, which is shown at the bottom of this page, for the tetrahedral angularity $\mathbb{A}(\mathcal{V}, \mathcal{A}, p)$ where $K_{\mathbb{A}} \in \mathbb{R}^{3n \times 6}$. Then, one has the following lemma.

Lemma 2: For the tetrahedral angularity $\mathbb{A}(\mathcal{V}, \mathcal{A}, p)$, one has *Span*$\{K_{\mathbb{A}}\} \subseteq$ *Null*$(R_{\mathcal{A}^*}) \subseteq$ *Null*$(R_{\mathcal{A}})$ and *Rank*$(R_{\mathcal{A}}) \leq$ *Rank*$(R_{\mathcal{A}^*}) \leq 3n - 6$.

Proof: According to Lemma 1, all the column vectors of $K_{\mathbb{A}}$ are in the null space of $R_{\mathcal{A}}$ and $R_{\mathcal{A}^*}$. Since $R_{\mathcal{A}}$ is a sub-matrix of $R_{\mathcal{A}^*}$ and they have the same number of columns, one has $\text{Rank}(R_{\mathcal{A}}) \leq \text{Rank}(R_{\mathcal{A}^*})$ and $\text{Null}(R_{\mathcal{A}^*}) \subseteq \text{Null}(R_{\mathcal{A}})$. Since all

$$\begin{bmatrix} 1 & 0 & 0 & 1 & 0 & 0 & \cdots & 1 & 0 & 0 \\ 0 & 1 & 0 & 0 & 1 & 0 & \cdots & 0 & 1 & 0 \\ 0 & 0 & 1 & 0 & 0 & 1 & \cdots & 0 & 0 & 1 \\ p_1(1) & p_1(2) & 0 & p_2(1) & p_2(2) & 0 & \cdots & p_n(1) & p_n(2) & 0 \\ -p_1(2) & p_1(1) & 0 & -p_2(2) & p_2(1) & 0 & \cdots & -p_n(2) & p_n(1) & 0 \\ p_1(1) & p_1(2) & p_1(3) & p_2(1) & p_2(2) & p_2(3) & \cdots & p_n(1) & p_n(2) & p_n(3) \end{bmatrix}^\top \tag{26}$$

the six column vectors of $K_{\mathbb{A}}$ are linearly independent, one has $\text{Rank}(R_{\mathcal{A}^*}) \leq 3n-6$. ■

Remark 1: It is worth noting that if $p=[p_1^\top,p_2^\top,p_3^\top,p_4^\top]^\top$ is the combination of translation, scaling and Z-axis rotation with respect to $p'=[p_1^{'\top},p_2^{'\top},p_3^{'\top},p_4^{'\top}]^\top$, then one always has $f^{\triangle_{1234}}(\alpha^*(p),p')=0$. However, the converse of the above argument is not true because $\{f_1=0,f_2=0,f_3=0\}$ is only a sufficient condition for (16). As such, $f^{\triangle_{1234}}(\alpha^*(p),p')=0$ and that p is a combination of translation, scaling and Z-axis rotation with respect to p' are not equivalent.

Next, we develop localizability conditions for sensor networks described by tetrahedral angularities in 3D.

IV. Localizability Conditions

Before giving localizability conditions, we first formulate the angle-only network localization problem to be solved. We say nodes i,j,k are neighboring nodes of one another if $(i,j,k)\in\mathcal{A}$.

Problem 1: Consider a 3D sensor network described by a tetrahedral angularity $\mathbb{A}(\mathcal{V},\mathcal{A},p)$ where $\mathcal{V}=\mathcal{V}_a\cup\mathcal{V}_f$, $n_a\geq 2$, and for each tetrahedron $\mathcal{S}_{\triangle_{ijkm}}\in\mathcal{A}$, at least one of i,j,k,m has the knowledge of the direction of global Z-axis. Given anchor nodes' positions p_a in $\sum_g$, the aim is to determine the positions of the free nodes p_f using the nodes' angle measurements with respect to their neighbors and the communication of estimated positions with their neighbors.

Denote by $\hat{p}=[\hat{p}_a^\top,\hat{p}_f^\top]^\top\in\mathbb{R}^{3n}$ the estimation of all nodes' positions. Since each tetrahedral angle subset in $\mathcal{A}$ will give one angle-induced linear constraint (19), the formulated localization Problem 1 is equivalent to finding $\hat{p}_f$ subject to

$$
\begin{aligned}
&f^{\triangle_{ijkm}}(\alpha^*,\hat{p})=A^{\triangle_{ijkm}}(\alpha^*)\hat{p}_i+B^{\triangle_{ijkm}}(\alpha^*)\hat{p}_j\\
&+C^{\triangle_{ijkm}}(\alpha^*)\hat{p}_k+D^{\triangle_{ijkm}}(\alpha^*)\hat{p}_m=0,\forall\mathcal{S}_{\triangle_{ijkm}}\in\mathcal{A}\\
&\hat{p}_i=p_i,\forall i\in\mathcal{V}_a,
\end{aligned}
\tag{27}
$$

where the angles in $A^{\triangle_{ijkm}}(\alpha^*)$, $B^{\triangle_{ijkm}}(\alpha^*)$, $C^{\triangle_{ijkm}}(\alpha^*)$, $D^{\triangle_{ijkm}}(\alpha^*)$ are constants and can be obtained using the nodes' angle measurements. Note that $\mathcal{T}(\mathcal{V},\mathcal{A})$ represents both the measurement topology and communication topology. Then, we can define localizable angularity.

Definition 1: A tetrahedral angularity $\mathbb{A}(\mathcal{V},\mathcal{A},p)$ is said to be *localizable* if the solution $\hat{p}_f$ to (27) is unique and $\hat{p}_f=p_f$.

In the follow-up subsections, we investigate the algebraic and topological localizability conditions, respectively.

A. Algebraic Localizability Condition

Now, we develop algebraic localizability conditions for tetrahedral angularities $\mathbb{A}(\mathcal{V},\mathcal{A},p)$. We transfer the localization problem (27) into a least-square optimization problem by defining the cost function of the angle-only network localization Problem 1 as

$$
\begin{aligned}
J(\hat{p})&=\sum\nolimits_{\mathcal{S}_{\triangle_{ijkm}}\in\mathcal{A}}\|f^{\triangle_{ijkm}}(\alpha^*,\hat{p})\|^2\\
&=\sum\nolimits_{\mathcal{S}_{\triangle_{ijkm}}\in\mathcal{A}}\|A^{\triangle_{ijkm}}(\alpha^*)\hat{p}_i+B^{\triangle_{ijkm}}(\alpha^*)\hat{p}_j\\
&\quad+C^{\triangle_{ijkm}}(\alpha^*)\hat{p}_k+D^{\triangle_{ijkm}}(\alpha^*)\hat{p}_m\|^2,
\end{aligned}
\tag{28}
$$

where $\hat{p}_i=p_i,\forall i\in\mathcal{V}_a$. Our aim is to obtain the localizability condition, under which the true position p_f is the unique and global minimizer of (28). According to the definition of the angle measurement matrix in (25), the cost function defined in (28) can be rewritten as

$$
J(\hat{p})=\hat{p}^\top R_{\mathcal{A}}^\top(\alpha^*)R_{\mathcal{A}}(\alpha^*)\hat{p}. \tag{29}
$$

Let $\mathcal{L}(\alpha^*):=R_{\mathcal{A}}^\top(\alpha^*)R_{\mathcal{A}}(\alpha^*)\in\mathbb{R}^{3n\times 3n}$. By partitioning matrix $R_{\mathcal{A}}=[R_{\mathcal{A}}^aR_{\mathcal{A}}^f]$ into anchor nodes' part $R_{\mathcal{A}}^a\in\mathbb{R}^{6n_{\mathcal{A}}^{\triangle}\times 3n_a}$ and free nodes' part $R_{\mathcal{A}}^f\in\mathbb{R}^{6n_{\mathcal{A}}^{\triangle}\times 3n_f}$, the matrix $\mathcal{L}(\alpha^*)$ can be written in the form of

$$
\mathcal{L}(\alpha^*)=\begin{bmatrix}\mathcal{L}_{aa} & \mathcal{L}_{af}\\ \mathcal{L}_{fa} & \mathcal{L}_{ff}\end{bmatrix}, \tag{30}
$$

where $\mathcal{L}_{aa}=(R_{\mathcal{A}}^a)^\top R_{\mathcal{A}}^a\in\mathbb{R}^{3n_a\times 3n_a}$, $\mathcal{L}_{af}=(R_{\mathcal{A}}^a)^\top R_{\mathcal{A}}^f\in\mathbb{R}^{3n_a\times 3n_f}$, $\mathcal{L}_{fa}=(R_{\mathcal{A}}^f)^\top R_{\mathcal{A}}^a\in\mathbb{R}^{3n_f\times 3n_a}$, and $\mathcal{L}_{ff}=(R_{\mathcal{A}}^f)^\top R_{\mathcal{A}}^f\in\mathbb{R}^{3n_f\times 3n_f}$.

Lemma 3: If $\hat{p}_f^*$ is a minimizer of the cost function (28), then it is also a global minimizer and $\mathcal{L}_{ff}\hat{p}_f^*+\mathcal{L}_{fa}p_a=0$.

Proof: Substituting (30) into (29) yields

$$
J(\hat{p})=\tilde{J}(\hat{p}_f)=p_a^\top\mathcal{L}_{aa}p_a+2p_a^\top\mathcal{L}_{af}\hat{p}_f+\hat{p}_f^\top\mathcal{L}_{ff}\hat{p}_f, \tag{31}
$$

where we used the fact $\hat{p}_a=p_a$. Then, any minimizer of (31) satisfies $\nabla_{\hat{p}_f^*}\tilde{J}(\hat{p}_f^*)=\mathcal{L}_{ff}\hat{p}_f^*+\mathcal{L}_{fa}p_a=0$. Also, it follows from [22] that $\hat{p}_f^*$ is a global minimizer. This is because if we assume $\hat{p}_f^*=p_f+\delta p_f$ where $\delta p_f\in\mathbb{R}^{3n_f}$, then one has from $\mathcal{L}(\alpha^*)p=0$ and $J(\hat{p}^*)=(p+[0;\delta p_f])^\top\mathcal{L}(\alpha^*)(p+[0;\delta p_f])=(\delta p_f)^\top\mathcal{L}_{ff}\delta p_f=0$ that $\delta p_f=0$. ■

Theorem 1: A tetrahedral angularity $\mathbb{A}(\mathcal{V},\mathcal{A},p)$ with $n_a\geq 2$ is localizable if and only if $\mathcal{L}_{ff}$ is nonsingular. When the angularity is localizable, the true positions of the free nodes can be calculated by $p_f=-\mathcal{L}_{ff}^{-1}\mathcal{L}_{fa}p_a$.

The proof of Theorem 1 is straightforward using Lemma 3 and [22]. Now, we derive conditions such that $\mathcal{L}_{ff}$ is nonsingular.

Theorem 2: For a tetrahedral angularity $\mathbb{A}(\mathcal{V},\mathcal{A},p)$ with $n_a\geq 2$, if *Rank*$(R_{\mathcal{A}}(\alpha))=3n-6$, then $\mathcal{L}_{ff}$ is nonsingular.

Proof: The rank condition $\text{Rank}(R_{\mathcal{A}}(\alpha))=3n-6$ implies that $R_{\mathcal{A}}(\alpha)$ has $3n-6$ linearly independent rows. Since the number of free nodes is less than $n-2$ and each free node has three degrees of freedom, the total number of degrees of freedom in p_f is less than $3n-6$. Due to the fact that $R_{\mathcal{A}}(\alpha)p=0$ can provide $3n-6$ independent linear equations, p_f can be uniquely determined by these linear equations. When p_f is uniquely determined (i.e., the angularity is localizable), one has from Theorem 1 that $\mathcal{L}_{ff}$ is nonsingular. ■

Theorem 2 provides a sufficient condition for the localizability of tetrahedral angularities. Now, we give a necessary and sufficient condition for the network localizability when $n_a = 2$.

Proposition 1: A tetrahedral angularity $\mathbb{A}(\mathcal{V}, \mathcal{A}, p)$ with $n_a = 2$ is localizable if and only if $Rank(R_{\mathcal{A}}(\alpha)) = 3n - 6$.

Proof: The sufficient part of this proposition is proved by Theorem 2. For the necessary part, if $\mathcal{L}_{ff}$ is nonsingular, then $\text{Rank}(\mathcal{L}_{ff}) = \text{Rank}(R^f_{\mathcal{A}}) = 3n - 6$. Since $R^f_{\mathcal{A}}$ is a submatrix of $R_{\mathcal{A}}$ and $\text{Rank}(R_{\mathcal{A}}(\alpha)) \leq 3n - 6$, one has $\text{Rank}(R_{\mathcal{A}}(\alpha)) = 3n - 6$. ■

For sensor networks described by tetrahedral angularities, to check their network localizability by the algebraic condition developed in Theorem 2, one needs to collect all the free nodes' measured angle information via communication channels. Inspired by [27], we now provide a method to check the networks' localizability in a distributed manner. Consider that the tetrahedral angularity $\mathbb{A}(\mathcal{V}, \mathcal{A}, p)$ has two anchor nodes in $\mathcal{V}_a = \{1, 2\}$, and $n - 2$ free nodes in $\mathcal{V}_f = \{3, 4, \ldots, n\}$. Based on the results of checking localizability in a distributed manner for 2D networks [27, Theorem 3.1], we can similarly have the following results for 3D networks.

Lemma 4: The 3D tetrahedral angularity $\mathbb{A}$ with $n_a = 2$ is localizable if and only if $Null(\mathcal{L}_{ff}) \perp E_{i-2}, \forall i \in \mathcal{V}_f$, where $E_{i-2} = e_{i-2} \otimes I_3$ and $e_{i-2} \in \mathbb{R}^{n-2}$ is the natural basis of $\mathbb{R}^{n-2}$, i.e., e_{i-2} is the column vector whose $(i-2)$th entry is 1 and all the other entries are zero.

Proof: Writing $\text{Null}(\mathcal{L}_{ff}) \perp E_{i-2}, \forall i \in \mathcal{V}_f$ into a compact form yields $\text{Null}(\mathcal{L}_{ff}) \perp I_{3(n-2)}$. Since $I_{3(n-2)}$ expands the entire Euclidean space $\mathbb{R}^{3(n-2)}$, $\text{Null}(\mathcal{L}_{ff}) \perp I_{3(n-2)}$ implies that $\text{Null}(\mathcal{L}_{ff}) = \emptyset$, that is to say $\mathcal{L}_{ff}$ is nonsingular. According to Theorem 1, the angularity is localizable if and only if $\mathcal{L}_{ff}$ is nonsingular, which completes the proof. ■

From the definition of E_{i-2}, one has that to check the condition $\text{Null}(\mathcal{L}_{ff}) \perp E_{i-2}$ for a specific node $i \in \mathcal{V}_f$, the node i only needs to know the $(3(i-2)-2)$th, $(3(i-2)-1)$th, and $3(i-2)$th components of every eigenvector of $\mathcal{L}_{ff}$. It is worth noting that node i can obtain these information by employing the distributed orthogonal iteration algorithm in [27, Algorithm 2]. Therefore, the 3D network's localizability can be checked in a distributed manner by following Lemma 4 and [27, Algorithm 2]. Indeed, the communication cost of this checking is high since several steps in each iteration of [27, Algorithm 2] require inter-node communication for checking localizability in a distributed manner.

B. Topological Localizability Condition

Due to the inequivalence mentioned in Remark 1, it is challenging to develop necessary and sufficient topological localizability conditions (relying on $\mathcal{T}(\mathcal{V}, \mathcal{A})$ only) for Problem 1 using the tool of rigidity graph theory. Instead, we now propose a sufficient topological localizability condition.

Theorem 3: For a tetrahedral angularity $\mathbb{A}(\mathcal{V}, \mathcal{A}, p)$ with $n_a = 2$, if $\mathcal{S}_{\triangle_{i(i+1)(i+2)(i+3)}} \in \mathcal{A}, \forall i = 1, \ldots, n-3$, and each tetrahedra in $\mathcal{A}$ is non-coplanar, then $\mathbb{A}$ is localizable.

Proof: For the first tetrahedron $\triangle 1234$, since nodes 1 and 2 are anchor nodes and the linear constraint (19) gives six linearly independent equations, the positions of nodes 3 and 4 can be localized according to Proposition 1. Then, given the second tetrahedron $\triangle 2345$, node 5 can be localized. Using the same reasoning sequentially for the remaining free nodes, the tetrahedral constraints in $\mathcal{A}$ can localize all the free nodes. ■

In Theorem 3, $\mathcal{A}$ contains at least $n-3$ tetrahedra, in which at least $n-3$ nodes need to have the knowledge of the global Z-axis. For an arbitrary tetrahedral angularity $\mathbb{A}(\mathcal{V}, \mathcal{A}, p)$, the number $n_Z \in \mathbb{N}^+$ of nodes required to know the global Z-axis is equal to the number $n^{\triangle}_{\mathcal{A}}$ of tetrahedra in $\mathcal{A}$. Since some tetrahedra in $\mathbb{A}$ have common nodes which have the knowledge of the global Z direction, the number of nodes required to have the knowledge of global Z direction can be reduced by sharing these common nodes. However, an inappropriate assignment of these global Z-axis nodes may induce large communication burden. Therefore, to avoid large communication burden, even distribution of the global Z-axis nodes is favored for engineering practices. Suppose the maximum number of neighboring nodes that each global Z-axis node can have is $n_{\max} \in \mathbb{N}^+$. To guarantee that each tetrahedron contains one global Z-axis node, at least $\lceil \frac{n}{n_{\max}+1} \rceil$ global Z-axis nodes are needed. To evenly distribute the communication burden, a combinatorial task assignment algorithm [28, Chapters 9 and 19] can be employed to construct the tetrahedral angle set $\mathcal{A}$ such that $\mathbb{A}$ is localizable and that the number of each global Z-axis node's neighbors is less than $n_{\max}$.

V. Distributed Localization

In this section, we design distributed localization algorithms to estimate the positions of the free nodes under three cases, namely, continuous communication, aperiodic communication, and aperiodic communication on jointly localizable angularities, respectively.

A. Localization Under Continuous Communication

Based on the formulation of the least-square optimization problem given in (28), we design a gradient descent continuous localization algorithm

$$\dot{\hat{p}}_f(t) = -\nabla_{\hat{p}_f} \tilde{J}(\hat{p}_f) = -\mathcal{L}_{ff}\hat{p}_f(t) - \mathcal{L}_{fa}p_a \tag{32}$$

whose component form for each free node $i \in \mathcal{V}_f$ is

$$\begin{aligned}\dot{\hat{p}}_i(t) = &-\sum\nolimits_{\mathcal{S}_{\triangle_{ij_1k_1m_1}} \in \mathcal{A}} (A^{\triangle_{ij_1k_1m_1}}(\alpha^*))^\top \\ &\times f^{\triangle_{ij_1k_1m_1}}(\alpha^*, \hat{p}) \\ &-\sum\nolimits_{\mathcal{S}_{\triangle_{i_2j_2k_2m_2}} \in \mathcal{A}} (B^{\triangle_{j_2ik_2m_2}}(\alpha^*))^\top f^{\triangle_{j_2ik_2m_2}}(\alpha^*, \hat{p}) \\ &-\sum\nolimits_{\mathcal{S}_{\triangle_{j_3k_3im_3}} \in \mathcal{A}} (C^{\triangle_{j_3k_3im_3}}(\alpha^*))^\top f^{\triangle_{j_3k_3im_3}}(\alpha^*, \hat{p})\end{aligned}$$

$$- \sum_{\mathcal{S}_{\triangle_{j_4 k_4 m_4 i}} \in \mathcal{A}} (D^{\triangle_{j_4 k_4 m_4 i}}(\alpha^*))^\top f^{\triangle_{j_4 k_4 m_4 i}}(\alpha^*, \hat{p}) \tag{33}$$

where $f^{\triangle_{ij_1k_1m_1}}(\alpha^*, \hat{p}) = A^{\triangle_{ij_1k_1m_1}}(\alpha^*)\hat{p}_i(t) + B^{\triangle_{ij_1k_1m_1}}(\alpha^*)\hat{p}_{j_1}(t) + C^{\triangle_{ijkm}}(\alpha^*)\hat{p}_{k_1}(t) + D^{\triangle_{ijkm}}(\alpha^*)\hat{p}_{m_1}(t)$, and the forms of $f^{\triangle_{j_2ik_2m_2}}, f^{\triangle_{j_3k_3im_3}}, f^{\triangle_{j_4k_4m_4i}}$ can be similarly obtained from (24), j_s, k_s, m_s are i's neighbors, $s = 1, 2, 3, 4$ and $\mathcal{S}_{\triangle_{ij_1k_1m_1}} \neq \mathcal{S}_{\triangle_{j_2ik_2m_2}} \neq \mathcal{S}_{\triangle_{j_3k_3im_3}} \neq \mathcal{S}_{\triangle_{j_4k_4m_4i}}$, $\hat{p}_j(t) = p_j, \forall j \in \mathcal{V}_a$, and the constant matrix $A^{\triangle_{ij_1k_1m_1}}(\alpha^*) \in \mathbb{R}^{6\times 3}$ is only related to the measured angles in $\triangle_{ij_1k_1m_1}$. Therefore, the localization law (33) is distributed and can be implemented using node i's one time angle measurements and communication to obtain α^*, and continuous communication to obtain $\hat{p}_{j_s}(t), \hat{p}_{k_s}(t), \hat{p}_{m_s}(t)$.

Theorem 4: For a tetrahedral angularity $\mathbb{A}(\mathcal{V}, \mathcal{A}, p)$ with $n_a \geq 2$, if *Rank*$(R_{\mathcal{A}}(\alpha)) = 3n - 6$, then $\hat{p}_f$ globally converges to p_f under the localization algorithm (33).

Proof: According to Theorems 1 and 2, $\mathcal{L}_{ff}$ is nonsingular and positive definite. Consider the candidate Lyapunov function $V_1(t) = 0.5\|p_f - \hat{p}_f(t)\|^2$ whose time-derivative is

$$\begin{aligned} \dot{V}_1(t) = & -(p_f - \hat{p}_f(t))^\top \mathcal{L}_{ff}(p_f - \hat{p}_f(t)) \\ \leq & -\lambda_{\min}(\mathcal{L}_{ff})\|p_f - \hat{p}_f(t)\|^2 = -2\lambda_{\min}(\mathcal{L}_{ff})V_1(t). \end{aligned}$$

Since $\lambda_{\min}(\mathcal{L}_{ff}) > 0$, $V_1(t) \leq V_1(0)e^{-2\lambda_{\min}(\mathcal{L}_{ff})t}$ and $\hat{p}_f(t)$ globally and exponentially converges to p_f. ■

The above proof implies that the localization error $\|p_f - \hat{p}_f(t)\|$ converges with at least the exponential rate $\lambda_{\min}(\mathcal{L}_{ff})$, which depends on not only the sensor nodes' locations p, but also the topology $\mathcal{A}$ according to the definitions in (25) and (30). Since the convergence rate determines the overall required communication, it is important if it can be tuned after p and $\mathcal{A}$ are given. This can be achieved by adding a gain in front of the localization law (32). More specifically, if the localization error $\|\tilde{p}_f(t)\|$ is required to be within 10% of the initial localization error $\|\tilde{p}_f(0)\|$ after $\tau > 0$ seconds, then one can achieve this performance by executing the localization algorithm

$$\dot{\hat{p}}_f(t) = -k_c\left(\mathcal{L}_{ff}\hat{p}_f(t) + \mathcal{L}_{fa}p_a\right) \tag{34}$$

where $k_c = \frac{ln10}{\tau\lambda_{\min}(\mathcal{L}_{ff})}$ is a number which can be communicated among the network with low communication cost. This is because the closed-loop dynamics $\dot{\tilde{p}}_f(t) = -k_c\mathcal{L}_{ff}\tilde{p}_f(t)$ of (34) implies $\|\tilde{p}_f(t)\| \leq \|\tilde{p}_f(0)\|e^{-k_c\lambda_{\min}(\mathcal{L}_{ff})t}$, where $\tilde{p}_f = \hat{p}_f - p_f$. Since the convergence rate can be tuned, we clarify that the *reduced communication* in this paper refers to the reduction of the required communication in each iteration instead of the overall required communication until convergence. This is also reasonable since each sensor has a limited communication bandwidth.

Now, we summarize the implementation of the localization law (33) into Algorithm 2.

Remark 2: Compared to the other 3D network localization algorithms where at least three anchor nodes are needed and each free node has at least four neighbors [11], [13], [14], [21], the proposed localization algorithm (33) allows the network to have only two anchor nodes, and each free node to have only three neighbors. These advantages of (33) come with the cost of one more sensing requirement, i.e., at least one node in each tetrahedron can sense the global Z direction.

Algorithm 2: Implementation of the Distributed Localization Law (33)

1. Each node i establishes tetrahedral sensing and communication units with its neighbors j, k, m (each tetrahedra contains at least one node having the knowledge of global Z axis).
2. Each node i confirms its order in the tetrahedra, which can be $\mathcal{S}_{\triangle_{ij_1k_1m_1}}$ (node i will sense the global Z direction), $\mathcal{S}_{\triangle_{j_2ik_2m_2}}$ (node j_2 will sense the global Z direction), $\mathcal{S}_{\triangle_{j_3k_3im_3}}$, and $\mathcal{S}_{\triangle_{j_4k_4m_4i}}$.
3: For the case $\mathcal{S}_{\triangle_{ij_1k_1m_1}}$, each node i receives the angle measurements of nodes j_1, k_1, m_1, and then constructs the angle-induced linear constraint following Algorithm 1.
4: For the cases $\mathcal{S}_{\triangle_{j_2ik_2m_2}}, \mathcal{S}_{\triangle_{j_3k_3im_3}}, \mathcal{S}_{\triangle_{j_4k_4m_4i}}$, each node i sends its angle measurements to nodes j_2, j_3, j_4, respectively. Then, j_2, j_3, j_4 construct their corresponding angle-induced linear constraints.
5: Each node i executes the localization law (33) by using the established angle-induced linear constraints with its neighbors and the estimation $\hat{p}_i(t), \hat{p}_j(t), j \in \mathcal{N}_i$.

Remark 3: For the designed localization algorithm (32), we consider that the angle measurements are subjected to an additional noise, and define $\hat{\mathcal{L}}_{ff} \in \mathbb{R}^{3n_f \times 3n_f}$ as the corresponding matrix with noisy angle measurements. Then, the localization algorithm (32) under the noisy angle measurements becomes

$$\dot{\hat{p}}_f(t) = -(\hat{\mathcal{L}}_{ff}\hat{p}_f(t) + \hat{\mathcal{L}}_{fa}p_a). \tag{35}$$

According to [20, Theorem 4.3] and [22, Theorem 5], if $\|\mathcal{L}_{ff} - \hat{\mathcal{L}}_{ff}\| \leq \lambda_{\min}(\mathcal{L}_{ff})$, then $\hat{\mathcal{L}}_{ff}$ is nonsingular and the estimated position $\hat{p}_f$ under (35) converges to $-\hat{\mathcal{L}}_{ff}^{-1}\hat{\mathcal{L}}_{fa}p_a$ whose distance with respect to the true position $-\mathcal{L}_{ff}^{-1}\mathcal{L}_{fa}p_a$ is bounded. Note that when one uses larger k_c to get fast convergence rate in (34), the error $\|\hat{p}_f - p_f\|$ between the estimated position $\hat{p}_f$ under noisy measurements and the true position p_f may become larger.

B. Localization Under Aperiodic Communication

In this part, we consider that the communication among the sensor nodes is in an aperiodic sampling way. By taking the first component in (33) as an example, the information of $f^{\triangle_{ij_1k_1m_1}}(\alpha^*, \hat{p}) = A^{\triangle_{ijkm}}(\alpha^*)\hat{p}_i + B^{\triangle_{ijkm}}(\alpha^*)\hat{p}_j + C^{\triangle_{ijkm}}(\alpha^*)\hat{p}_k + D^{\triangle_{ijkm}}(\alpha^*)\hat{p}_m$ needs sensor node i's one time sensor measurement and communication to obtain the interior angles α^*, and needs continuous communication to obtain $\hat{p}_j(t), \hat{p}_k(t), \hat{p}_m(t)$. Assume that the angle measurements of α^* are noise-free and precise, but the real-time communication of $\hat{p}_i, \hat{p}_j, \hat{p}_k, \hat{p}_m$ is in an aperiodic sampling way, under which only $\hat{p}_i(t_k), \hat{p}_j(t_k), \hat{p}_k(t_k), \hat{p}_m(t_k)$ are available for $t \in [t_k, t_{k+1})$. Also assume that all sensor nodes' sampling time instants $\{t_1, t_2, \ldots, t_k, \ldots\}$ are synchronized. Firstly, we give an assumption about the sampling interval.

Assumption 1: The aperiodic sampling interval satisfies

$$0 < (t_{k+1} - t_k) = \Delta_k = \Delta_0 + \tilde{\Delta}_k, \forall k = 1, \ldots, \infty, \quad (36)$$

where $\Delta_0 > 0$ is a fixed scalar, $\Delta_{\min} \leq \tilde{\Delta}_k \leq \Delta_{\max}, \forall k = 1, \ldots, \infty$, and $\Delta_{\min} > 0, \Delta_{\max} > 0$ are the lower and upper bounds of $\tilde{\Delta}_k$, respectively.

Defining $\hat{p}_f(t_k) = [\hat{p}_{n_a+1}^\top(t_k), \ldots, \hat{p}_n^\top(t_k)]^\top \in \mathbb{R}^{3n_f}$, we design a piece-wise continuous localization algorithm based on the aperiodically sampled information

$$\dot{\hat{p}}_f(t) = -\mathcal{L}_{ff}\hat{p}_f(t_k) - \mathcal{L}_{fa}p_a, t \in [t_k, t_{k+1}), \quad (37)$$

where $k = 1, \ldots, \infty$. Since $-\mathcal{L}_{ff}\hat{p}_f(t_k) - \mathcal{L}_{fa}p_a$ is constant for $t \in [t_k, t_{k+1})$, the state $\hat{p}_f(t_{k+1})$ under the control of (37) can be described by

$$\hat{p}_f(t_{k+1}) = \hat{p}_f(t_k) + \Delta_k(-\mathcal{L}_{ff}\hat{p}_f(t_k) - \mathcal{L}_{fa}p_a). \quad (38)$$

By defining estimation error $\tilde{p}_f(t_k) = \hat{p}_f(t_k) - p_f$, one has

$$\tilde{p}_f(t_{k+1}) = (I - \Delta_k\mathcal{L}_{ff})\tilde{p}_f(t_k). \quad (39)$$

For the special case of periodic sampling $\Delta_k = \Delta_0, \forall k = 1, \ldots, \infty$, one directly has the conclusion that if $\Delta_0 < 2\lambda_{\max}^{-1}(\mathcal{L}_{ff})$, then $\tilde{p}_f(t_k) \to 0$ as $k \to \infty$. For the general case of aperiodic sampling, (39) can be rewritten as

$$\tilde{p}_f(t_{k+1}) = (I - \Delta_0\mathcal{L}_{ff})\tilde{p}_f(t_k) - \tilde{\Delta}_k\mathcal{L}_{ff}\tilde{p}_f(t_k). \quad (40)$$

To analyze the stability of the system (40), we employ the tool of the small-gain theorem[29, Section 5.4]. According to [30] and [31, Lemma 2], one has the following lemma.

Lemma 5: For all $\Delta_{\min} \leq \Delta_k \leq \Delta_{\max}$ in (40), if the spectral radius $\rho(I - \Delta_0\mathcal{L}_{ff}) < 1$ and $\|\tilde{\Delta}_k\mathcal{L}_{ff}\|_\infty \leq 1$, then there exists a matrix $0 < P = P^\top \in \mathbb{R}^{3n_f \times 3n_f}$ such that for every $k \in \mathbb{N}^+$,

$$(I - \Delta_k\mathcal{L}_{ff})^\top P(I - \Delta_k\mathcal{L}_{ff}) - P < 0 \quad (41)$$

Note that Lemma 5 provides a sufficient condition for the selection of Δ_0 and Δ_k such that (41) holds. Now, we give the main results for the case of aperiodic communication.

Theorem 5: For a tetrahedral angularity $\mathbb{A}(\mathcal{V}, \mathcal{A}, p)$ with $n_a \geq 2$ and $Rank(R_{\mathcal{A}}(\alpha)) = 3n - 6$, if $\rho(I - \Delta_0\mathcal{L}_{ff}) < 1$ and $\|\tilde{\Delta}_k\mathcal{L}_{ff}\|_\infty \leq 1$, then under the aperiodic communication series $\{t_k\}$ and the localization algorithm (37), $\hat{p}_f(t)$ globally converges to p_f.

Proof: Design a Lyapunov function candidate

$$V_2(k) = \tilde{p}_f^\top(t_k)P\tilde{p}_f(t_k) > 0 \quad (42)$$

which is positive definite and radially unbounded. According to the conditions in Lemma 5 and (41), one has

$$\begin{aligned} &V_2(k+1) - V_2(k) \\ &= \tilde{p}_f^\top(t_k)[(I - \Delta_k\mathcal{L}_{ff})^\top P(I - \Delta_k\mathcal{L}_{ff}) - P]\tilde{p}_f(t_k) < 0 \end{aligned}$$

which implies that $\tilde{p}_f(t_k) \to 0$ globally as $k \to \infty$. ■

Note that similar to (34), one can also add a positive gain in front of (37) to tune the convergence rate of (42), i.e.,

$$\dot{\hat{p}}_f(t) = -k_c(\mathcal{L}_{ff}\hat{p}_f(t_k) + \mathcal{L}_{fa}p_a), t \in [t_k, t_{k+1}), \quad (43)$$

where $k_c > 0$ and needs to satisfy $\rho(I - k_c\Delta_0\mathcal{L}_{ff}) < 1$ and $\|k_c\tilde{\Delta}_k\mathcal{L}_{ff}\|_\infty \leq 1$ according to Lemma 5.

C. Localization Under Aperiodic Communication for Jointly Localizable Angularities

For the case of aperiodic communication investigated in the previous subsection, each node needs to communicate with all of its neighbors at each sampling instant. To further reduce the communication burden for the network, we consider in this subsection that each node only needs to communicate with a portion of its neighbors at each sampling instant, and communicate with each neighbor one time over a period of time. It has been shown in [24] that the unavailability of neighbors' estimated positions at some sampling instants can make a stable localization network unstable. To study this case, we firstly define a matrix $\mathcal{L}_{ff}^{t_k} \in \mathbb{R}^{3n_f \times 3n_f}$ which represents the part in $\mathcal{L}_{ff}$ whose corresponding communication links among the free nodes are available at $t = t_k$, more explicitly,

$$\mathcal{L}_{ff}^{t_k}[i,j] = \begin{cases} \mathcal{L}_{ff}[i,j], \text{if the communication between} \\ \qquad \text{the free node } i + n_a \text{ and node } j + n_a \\ \qquad \text{is available at } t = t_k \\ 0, \quad \text{otherwise} \end{cases}$$

where $1 \leq i, j \leq n_f$, and $\mathcal{L}_{ff}[i,j]$ represents the block of the matrix $\mathcal{L}_{ff}$'s $(3i-2)$th $\sim (3i)$ th rows and $(3j-2)$th $\sim (3j)$ th columns. Then, we define jointly localizable angularities.

Definition 2: For $m \in \mathbb{N}^+$ and an angularity $\mathbb{A}(\mathcal{V}, \mathcal{A}, p)$ with fixed communication topology described by $\mathcal{A}$, we say $\mathbb{A}$ is m-jointly localizable if for every $k \in \mathbb{N}, \sum_{i=k}^{k+m} \mathcal{L}_{ff}^{t_i} = \mathcal{L}_{ff}$ and $\mathcal{L}_{ff}$ is nonsingular.

For the case $m = 2$, we propose the following localization algorithm for a 2-jointly localizable angularity $\mathbb{A}(\mathcal{V}, \mathcal{A}, p)$

$$\dot{\hat{p}}_f(t) = -\mathcal{L}_{ff}^{t_k}\hat{p}_f(t_k) - \mathcal{L}_{ff}^{t_{k-1}}\hat{p}_f(t_{k-1}) - \mathcal{L}_{fa}p_a, t \in [t_k, t_{k+1}) \quad (44)$$

where $\mathcal{L}_{ff}^{t_k} + \mathcal{L}_{ff}^{t_{k-1}} = \mathcal{L}_{ff}, \mathcal{L}_{ff}^{t_{k-1}} = (\mathcal{L}_{ff}^{t_{k-1}})^\top \neq 0$, and $\mathcal{L}_{ff}^{t_k} = (\mathcal{L}_{ff}^{t_k})^\top \neq 0$. The intuition of the localization algorithm (44) is that if sensor node i cannot receive its neighboring node j's estimation $\hat{p}_j$ at $t = t_k$, then node i will use node j's last time estimation $\hat{p}_j(t_{k-1})$ to continue the iteration of the network localization process. Based on (44), the position estimation error $\tilde{p}_f$ at $t = t_{k+1}$ can be written as

$$\begin{aligned} \tilde{p}_f(t_{k+1}) &= \hat{p}_f(t_k) + [-\mathcal{L}_{ff}^{t_k}\hat{p}_f(t_k) \\ &\quad - \mathcal{L}_{ff}^{t_{k-1}}\hat{p}_f(t_{k-1}) - \mathcal{L}_{fa}p_a]\Delta_k - p_f \\ &= (I - \Delta_k\mathcal{L}_{ff})\tilde{p}_f(t_k) + \Delta_k\mathcal{L}_{ff}^{t_{k-1}}\left(\tilde{p}_f(t_k) - \tilde{p}_f(t_{k-1})\right), \end{aligned} \quad (45)$$

where we have used the fact $\hat{p}_f(t_k) - \hat{p}_f(t_{k-1}) = \tilde{p}_f(t_k) - \tilde{p}_f(t_{k-1})$. Since $\Delta_k = \Delta_0 + \tilde{\Delta}_k$, (45) can be rewritten as

$$\begin{bmatrix} \tilde{p}_f(t_{k+1}) \\ \tilde{p}_f(t_k) \end{bmatrix} = H_1 \begin{bmatrix} \tilde{p}_f(t_k) \\ \tilde{p}_f(t_{k-1}) \end{bmatrix} + H_2 \begin{bmatrix} \tilde{p}_f(t_k) \\ \tilde{p}_f(t_{k-1}) \end{bmatrix}, \tag{46}$$

where $H_1 = \begin{bmatrix} I - \Delta_0 \mathcal{L}_{ff} & 0 \\ I & 0 \end{bmatrix} \in \mathbb{R}^{6n_f \times 6n_f}$ and $H_2 = \begin{bmatrix} \Delta_k \mathcal{L}_{ff}^{t_{k-1}} - \tilde{\Delta}_k \mathcal{L}_{ff} & -\Delta_k \mathcal{L}_{ff}^{t_{k-1}} \\ 0 & 0 \end{bmatrix} \in \mathbb{R}^{6n_f \times 6n_f}$. Now, we have the results for the localization of 2-jointly localizable angularities.

Theorem 6: For a tetrahedral and 2-jointly localizable angularity $\mathbb{A}(\mathcal{V}, \mathcal{A}, p)$ with $n_a \geq 2$, if $\rho(H_1) < 1$ and $\|H_2\|_\infty \leq 1$, then under the localization algorithm (44), $\hat{p}_f(t)$ globally converges to p_f.

Proof: Following Lemma 5, if $\rho(H_1) < 1$ and $\|H_2\|_\infty \leq 1$, then one has $\|\tilde{p}_f(t_{k+1})\| < \|\tilde{p}_f(t_{k-1})\|$. Although some nodes do not have all their neighboring nodes' estimated positions at $t = t_k$, the estimation error $\|\tilde{p}_f(t)\|$ at the sampling time $t = t_{k+1}$ is always less than the estimation error $\|\tilde{p}_f(t)\|$ at the sampling time $t = t_{k-1}$, i.e., the estimation error will become smaller and smaller as $t \to \infty$. Using a similar same Lyapunov function candidate as $V_2(k)$ for the dynamics (46), one has that $\hat{p}_f(t)$ globally converges to p_f. ■

Following the same design procedure, the results can be straightforwardly extended to the case of an arbitrary m-jointly localizable angularity.

Remark 4: Note that $\mathcal{L}_{ff}^{t_k}$ and $\mathcal{L}_{ff}^{t_{k-1}}$ are constant matrices for all sampling instants which can be determined before the execution of the localization algorithm. Therefore, given the bounds of $\Delta_0, \tilde{\Delta}_k$ and the angle measurement matrix $R_{\mathcal{A}}(\alpha)$, the stability conditions in Theorems 5–6 can be checked and the execution of the localization algorithms (37), (44) is distributed. In addition, different from the proposed strategy in [24] where all the communication data and iteration at $t = t_k$ will be discarded if there is one node at $t = t_k$ that cannot receive its all neighbors' estimated positions, our proposed strategy will use the latest received estimated positions from neighbors to continue the iteration of the localization process.

Remark 5: Multi-agent formation control problem is a dual problem of network localization. The proposed localization approach in this paper can be used to achieve multi-agent formation control. More specifically, by replacing the anchor nodes by leaders, free nodes by followers, and estimation $\hat{p}_i$ in (33) by follower i's position p_i, a desired angle-described formation can be achieved by using relative position measurements.

Remark 6: Compared to distance measurement technologies which are usually active, an angle measurement usually is passive since its sensing based on cameras mainly relies on environmental light and there is no need to transmit a detection signal. Thus, less power consumption is usually needed for angle measurements. There are generally two types of angle measurement technologies. The first is vision-based, where the angles formed with neighboring nodes are calculated from cameras' images. The second is via directional antenna arrays. For example, the Bluetooth 5.1 technology has enabled acceptable angle measurements in realistic scenarios [32]. In addition, the capability of acquiring Z-axis knowledge can be empowered by equipping the sensor node with a gravity sensor, or an inertial measurement unit, or extracting the gravity direction via image processing [33], which usually is energy-efficient and low-cost.

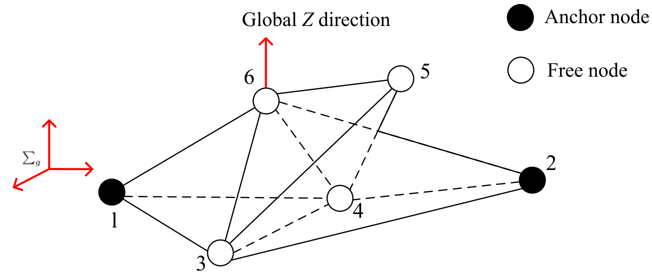

Fig. 2. Sensor network with 2 anchor nodes and 4 free nodes.

VI. Simulation Examples

In this section, we validate the theoretical results by localizing a sensor network formed by two anchor nodes and four free nodes. As shown in Fig. 2, the sensor network consists of three tetrahedra $\triangle 6134, \triangle 6345, \triangle 6234$. Among the four free nodes, only node 6 has the knowledge of the global Z direction and node 5 only has three neighbors. Following Section II-B, nodes 3, 4, 5 can measure the interior angles with respect to the their neighboring nodes. While node 6 can measure not only the interior angles, but also the angles formed between the global Z direction and the rays $\overrightarrow{6j}, j \in \{1, 2, 3, 4, 5\}$. The configuration of these sensor nodes is $p_1 = [0.1, 0.1, -0.1]^\top$, $p_2 = [0.2, 4.8, 0.6]^\top$, $p_3 = [-0.5, 1.0, -2.3]^\top$, $p_4 = [1.2, 3.0, -2.8]^\top$, $p_5 = [-2.2, 4.0, 1.0]^\top$, $p_6 = [-1.1, 2.4, 0.5]^\top$. From the simulation cases on different embedding p, if the two anchor nodes' Z coordinates are distinct and the three tetrahedra are non-coplanar, then the sensor network is always localizable, i.e., $\text{Rank}(\mathcal{L}_{ff}) = 12$. The free nodes' initial position estimations are $\hat{p}_3(0) = [3.2, 3.3, -4.5]^\top$, $\hat{p}_4(0) = [1.4, -1.5, -2.1]^\top$, $\hat{p}_5(0) = [-1.8, 0.3, 7.9]^\top$, $\hat{p}_6(0) = [-1.1, -3.2, 3.9]^\top$. We conduct five simulation cases corresponding to the localization algorithms (33), (35), (37), (44), and (43), respectively. Finally, we will compare their communication times among the nodes and convergence rate of the localization error.

A. Continuous Communication

For the case of continuous communication, we use Matlab/Simulink to simulate the continuous algorithm (33), where the Runge-Kutta method with fixed-step size 0.1 s is selected as the solver. The simulation result is shown in Fig. 3, from which one can see that the position estimation errors converge to zero within 300 seconds. Moreover, for the continuous case, according to the analysis for (34), one can find a proper gain k_c to achieve a desired convergence rate.

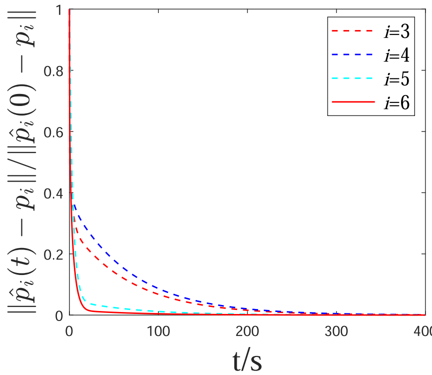

Fig. 3. Position estimation errors under algorithm (33).

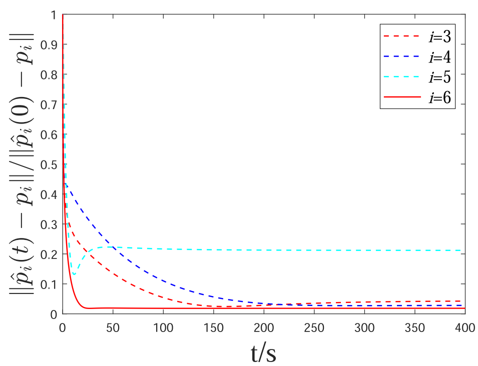

Fig. 4. Position estimation errors under algorithm (35).

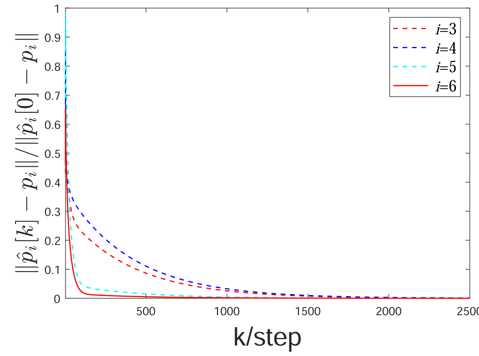

Fig. 5. Position estimation errors under algorithm (37).

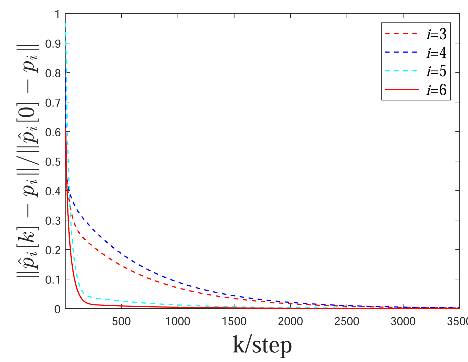

Fig. 6. Position estimation errors under algorithm (44).

B. Continuous Communication With Measurement Noise

In this case, we consider that the angle measurements in free nodes 3,4,5,6 are subjected to a random but constant angle measurement noise, which is bounded by 5°. By using the localization algorithm (35) in Remark 3, the simulation results are shown in Fig. 4, from which one can see that the position estimation errors converge to bounded values within 300 seconds. According to Remark 3, when angle measurement noise exists, the position estimation errors are bounded, which in this case is bounded by $\|\hat{p}_i(\infty) - p_i\| \leq 0.25\|\hat{p}_i(0) - p_i\|$.

C. Aperiodic Communication

For the case of aperiodic communication, the aperiodic sampling instants are selected as $k = 3 * i * T$ and $k = (3 * i + 2) * T, i = 1, 2, 3, \ldots, \infty$, where $T = 0.1$s. Then, under the aperiodic localization algorithm (37), the simulation result is shown in Fig. 5, from which one sees that the position estimation errors converge to zero within 2000 steps. Since the sampling period T is selected as 0.1 s, the required iteration steps for the convergence of position estimation errors will cost 2000*0.1=200 seconds.

D. Aperiodic Communication for a 2-Jointly Localizable Angularity

For the aperiodic communication, we still set the aperiodic sampling instants as $k = 3 * i * T$ and $k = (3 * i + 2) * T, i = 1, 2, 3, \ldots, \infty$, where $T = 0.1$s. The 2-jointly localizable angularity has the properties that

- when $k = 3 * i * T$, the communication links (3,4), (3,6), (5,6), and (4,5) are available.
- when $k = (3 * i + 2) * T$, the communication links (3,5) and (4,6) are available.

Then, under the aperiodic localization algorithm (44), the simulation result is shown in Fig. 6, from which one sees that the position estimation errors converge to zero within 3000 steps, i.e., 300 seconds. It is worth noting that the needed iteration steps in algorithm (44) is longer than that in algorithm (37), which implies the compromise of converge time/steps and communication cost.

E. Aperiodic Communication With Tuned Convergence Rate

To illustrate that the convergence rate of the aperiodic localization law (37) can also be tuned, we simulate the localization law (43). We choose the gain $k_c = 17$ and the sampling period $T = 0.01$s. The corresponding sampling frequency is 100 Hz, which is implementable in most of angle measurement sensors and on-board computers. The gain k_c is chosen such that the convergence rate can be faster and the stability conditions still hold. The simulation results are shown in Fig. 7, where the errors converge within 1000 steps, i.e., 10 seconds.

Now, we summarize the convergence time/steps and communication times in these simulation cases in Table I, where in each sampling instant of (37), we consider the network's communication times as 6 due to the existence of 6 links among

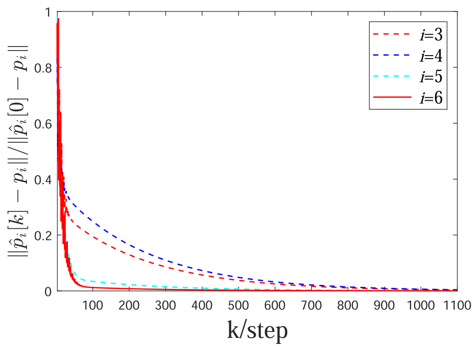

Fig. 7. Position estimation errors under algorithm (43).

TABLE I
COMPARISON OF DIFFERENT LOCALIZATION ALGORITHMS

Algorithms \ Properties	Iteration time or steps	Overall communication times till convergence
Continuous (33)	300 seconds	∞
Continuous (35)	300 seconds	∞
Aperiodic (37)	2000 steps/ 200 seconds	1.2×10^4
Aperiodic (44)	3000 steps/ 300 seconds	6×10^3
Aperiodic (43)	1000 steps/ 10 seconds	1.2×10^4

the 4 free nodes. The iteration time in Table I represents the cost time of the required iteration steps for the convergence of position estimation errors under the selected sampling period. We can see from Table I that the communication burden under the algorithm (44) is lighter than (33) and (37). If one uses those localization laws where each node needs 4 neighbors to localize the sensor network in Fig. 2, at least one more communication link needs to be added between node 5 and one of the other nodes, which requires more communication in each iteration than the localization laws in this paper.

VII. CONCLUSION

This paper has studied network localization problem for 3D tetrahedral angularities where each node can only measure interior angles towards its neighbors and at least one node in each tetrahedron has the knowledge of the global Z axis. Compared to the existing results where each node needs at least 4 neighbors to construct a linear constraint, we allow each node to only have 3 neighbors such that the communication burden can be reduced. Also, the network is only required to have 2 anchor nodes in comparison with the existing works which require at least 3 anchor nodes. Both algebraic and topological localizability conditions have been derived for the networks described by tetrahedral angularities. Three distributed localization algorithms have been designed under the cases of continuous communication, aperiodic communication, and aperiodic communication on jointly localizable angularities, respectively. Future work will focus on other communication factors, such as asynchronized sampling and communication delays.

REFERENCES

[1] A. Kleiner and C. Dornhege, "Real-time localization and elevation mapping within urban search and rescue scenarios," *J. Field Robot.*, vol. 24, no. 8–9, pp. 723–745, 2007.
[2] H. Wu, X. Mei, X. Chen, J. Li, J. Wang, and P. Mohapatra, "A novel cooperative localization algorithm using enhanced particle filter technique in maritime search and rescue wireless sensor network," *ISA Trans.*, vol. 78, pp. 39–46, 2018.
[3] R. Swaminathan, M. Nischt, and C. Kuhnel, "Localization based object recognition for smart home environments," in *Proc. IEEE Int. Conf. Multimedia Expo.*, 2008, pp. 921–924.
[4] X. Wang, S. Yuan, R. Laur, and W. Lang, "Dynamic localization based on spatial reasoning with RSSI in wireless sensor networks for transport logistics," *Sensors Actuators A: Phys.*, vol. 171, no. 2, pp. 421–428, 2011.
[5] L. Cheng, C. Wu, Y. Zhang, H. Wu, M. Li, and C. Maple, "A survey of localization in wireless sensor network," *Int. J. Distrib. Sensor Netw.*, vol. 8, no. 12, 2012, Art. no. 962523.
[6] F. Guo, Y. Fan, Y. Zhou, C. Xhou, and Q. Li, *Space Electronic Reconnaissance: Localization Theories and Methods*. New York, NY, USA: Wiley, 2014.
[7] X. Li, X. Luo, and S. Zhao, "Globally convergent distributed network localization using locally measured bearings," *IEEE Trans. Control Netw. Syst.*, vol. 7, no. 1, pp. 245–253, Mar. 2020.
[8] G. Mao, B. Fidan, and B. D. Anderson, "Wireless sensor network localization techniques," *Comput. Netw.*, vol. 51, no. 10, pp. 2529–2553, 2007.
[9] P. Biswas, T.-C. Liang, K.-C. Toh, Y. Ye, and T.-C. Wang, "Semidefinite programming approaches for sensor network localization with noisy distance measurements," *IEEE Trans. Automat. Sci. Eng.*, vol. 3, no. 4, pp. 360–371, Oct. 2006.
[10] J. Aspnes *et al.*, "A theory of network localization," *IEEE Trans. Mobile Comput.*, vol. 5, no. 12, pp. 1663–1678, Dec. 2006.
[11] X. Fang, X. Li, and L. Xie, "Angle-displacement rigidity theory with application to distributed network localization," *IEEE Trans. Autom. Control*, vol. 66, no. 6, pp. 2574–2587, Jun. 2021.
[12] X. Fang, X. Li, and L. Xie, "3-D distributed localization with mixed local relative measurements," *IEEE Trans. Signal Process.*, vol. 68, pp. 5869–5881, Oct. 2020.
[13] Z. Lin, "Theory and algorithms in distributed localization for multi-vehicle networks using graph Laplacian techniques," in *Cooperative Localization and Navigation Theory*, Boca Raton, FL, USA: CRC Press, 2019.
[14] K. Cao, Z. Han, Z. Lin, and L. Xie, "Bearing-only distributed localization: A unified barycentric approach," *Automatica*, vol. 133, 2021, Art. no. 109834.
[15] Y. Wang, G. Wang, S. Chen, K. Ho, and L. Huang, "An investigation and solution of angle based rigid body localization," *IEEE Trans. Signal Process.*, vol. 68, pp. 5457–5472, Sep. 2020.
[16] L. Chen, M. Cao, and C. Li, "Angle rigidity and its usage to stabilize multi-agent formations in 2-D," *IEEE Trans. Autom. Control*, vol. 66, no. 8, pp. 3667–3681, Aug. 2021.
[17] G. Jing, C. Wan, and R. Dai, "Angle-based sensor network localization," *IEEE Trans. Autom. Control*, vol. 67, no. 2, pp. 840–855, Feb. 2022.
[18] G. Wang, K. C. Ho, and X. Chen, "Bias reduced semidefinite relaxation method for 3-D rigid body localization using AOA," *IEEE Trans. Signal Process.*, vol. 69, pp. 3415–3430, Jun. 2021.
[19] Y. Diao, Z. Lin, and M. Fu, "A barycentric coordinate based distributed localization algorithm for sensor networks," *IEEE Trans. Signal Process.*, vol. 62, no. 18, pp. 4760–4771, Sep. 2014.
[20] Z. Lin, T. Han, R. Zheng, and M. Fu, "Distributed localization for 2-D sensor networks with bearing-only measurements under switching topologies," *IEEE Trans. Signal Process.*, vol. 64, no. 23, pp. 6345–6359, Dec. 2016.
[21] T. Han, Z. Lin, R. Zheng, Z. Han, and H. Zhang, "A barycentric coordinate based approach to three-dimensional distributed localization for wireless sensor networks," in *Proc. 13th IEEE Int. Conf. Control Automat.*, 2017, pp. 600–605.
[22] S. Zhao and D. Zelazo, "Localizability and distributed protocols for bearing-based network localization in arbitrary dimensions," *Automatica*, vol. 69, pp. 334–341, 2016.
[23] Z. Han, K. Guo, L. Xie, and Z. Lin, "Integrated relative localization and leader-follower formation control," *IEEE Trans. Autom. Control*, vol. 64, no. 1, pp. 20–34, Jan. 2019.

[24] L. Shi, Q. Liu, J. Shao, and Y. Cheng, "Distributed localization in wireless sensor networks under denial-of-service attacks," *IEEE Control Syst. Lett.*, vol. 5, no. 2, pp. 493–498, Apr. 2021.

[25] K. ı. I. Doğançay, "3D pseudolinear target motion analysis from angle measurements," *IEEE Trans. Signal Process.*, vol. 63, no. 6, pp. 1570–1580, Mar. 2015.

[26] L. Chen, "Angle rigidity graph theory and multi-agent formations," Ph.D. dissertation, Univ. Groningen, The Netherlands, 2021.

[27] Z. Lin, Z. Han, and M. Cao, "Distributed localization for multi-robot systems in presence of unlocalizable robots," in *Proc. 59th IEEE Conf. Decis. Control*, 2020, pp. 1550–1555.

[28] C. H. Papadimitriou and K. Steiglitz, *Combinatorial Optimization: Algorithms and Complexity*. New York, NY, USA: Courier Corporation, 1998.

[29] H. K. Khalil, *Nonlinear Systems*. vol. 3, Englewood Cliffs, NJ, USA: Prentice-Hall, 2002.

[30] P. P. Khargonekar, I. R. Petersen, and K. Zhou, "Robust stabilization of uncertain linear systems: Quadratic stabilizability and H/sup infinity/control theory," *IEEE Trans. Autom. Control*, vol. 35, no. 3, pp. 356–361, Mar. 1990.

[31] H. Liu, L. Cheng, M. Tan, and Z.-G. Hou, "Containment control of continuous-time linear multi-agent systems with aperiodic sampling," *Automatica*, vol. 57, pp. 78–84, 2015.

[32] G. Pau, F. Arena, Y. E. Gebremariam, and I. You, "Bluetooth 5.1: An analysis of direction finding capability for high-precision location services," *Sensors*, vol. 21, no. 11, 2021, Art. no. 3589.

[33] R. Kennedy and C. J. Taylor, "Network localization from relative bearing measurements," in *Proc. IEEE/RSJ Int. Conf. Intell. Robots Syst.*, 2014, pp. 149–156.

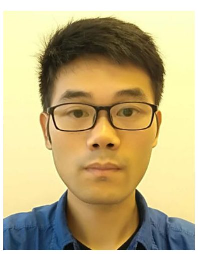

Liangming Chen received the B.E. degree in automation from Southwest Jiaotong University, Chengdu, China, in 2015. From 2015 to 2021, he has enrolled jointly in the Ph.D. programs with the Harbin Institute of Technology, Harbin, China, and the University of Groningen, Groningen, The Netherlands. He is currently a Research Fellow at the Nanyang Technological University, Singapore. His research interests include formation control, distributed localization, and aerial robotics.

Kun Cao received the B.Eng. degree in mechanical engineering from Tianjin University, Tianjin, China, in 2016, and the Ph.D. degree from the School of Electrical and Electronic Engineering, Nanyang Technological University, Singapore, in 2021. He is currently a Research Fellow with the latter. His research interests include localization, formation control, distributed optimization, and soft robotics.

Lihua Xie (Fellow, IEEE) received the Ph.D. degree in electrical engineering from the University of Newcastle, Callaghan, NSW, Australia, in 1992. Since 1992, he has been with the School of Electrical and Electronic Engineering, Nanyang Technological University, Singapore, where he is currently a Professor and the Director of the Center for Advanced Robotics Technology Innovation. He was the Head of the Division of Control and Instrumentation, and the Director of Delta-NTU Corporate Lab for Cyber-Physical Systems. His research interests include robust control and estimation, networked control systems, multiagent networks, localization, and unmanned systems. He is the Editor-in-Chief of *Unmanned Systems*. He was the Editor of the IET Book Series in Control and an Associate Editor for number of journals, including the IEEE TRANSACTIONS ON AUTOMATIC CONTROL, *Automatica*, IEEE TRANSACTIONS ON CONTROL SYSTEMS TECHNOLOGY, and IEEE TRANSACTIONS ON CONTROL OF NETWORK SYSTEMS. He was an IEEE Distinguished Lecturer and an Elected Member of Board of Governors with the IEEE Control System Society. He is a Fellow of IFAC and Fellow of the Academy of Engineering Singapore.

Xiaolei Li (Member, IEEE) received the B.Eng. and Ph.D. degrees in control engineering from Yanshan University, Qinhuangdao, China, in 2012 and 2018, respectively. Since September 2018, he has been a Research Fellow with the School of Electrical and Electronic Engineering, Nanyang Technological University, Singapore. His research interests include localization and formation control of robotic systems and cyber security of cyber-physical systems.

Mir Feroskhan received the Aerospace Engineering degree (with first-class Hons.) from Nanyang Technological University (NTU), Singapore, in 2011, and the Ph.D. degree in aerospace engineering from the Florida Institute of Technology, Melbourne, FL, USA, in 2016. He is currently an Assistant Professor with the School of Mechanical and Aerospace Engineering, NTU. His research interests include nonlinear control systems, VTOL systems, drone design and development, flight dynamics and control, and aerial robotics.